*Inorg. Chem.* **2008**, *47*, 9669−9683


# The Metal Loading Ability of β-Amyloid N-Terminus: A Combined Potentiometric and Spectroscopic Study of Copper(II) Complexes with β-Amyloid(1−16), Its Short or Mutated Peptide Fragments, and Its Polyethylene Glycol (PEG)-ylated Analogue

**Chiara A. Damante,[†] Katalin Ösz,[‡] Zoltán Nagy,[‡] Giuseppe Pappalardo,[§] Giulia Grasso,[§] Giuseppe Impellizzeri,[†] Enrico Rizzarelli,*[,†] and Imre Sóvágó*[,‡]**

*Department of Chemical Sciences, University of Catania, V.le A. Doria 6, 95125 Catania, Italy, Department of Inorganic and Analytical Chemistry, University of Debrecen, 4010 Debrecen, Hungary, and CNR Institute of Biostructures and Bioimaging, V.le A. Doria, 95125 Catania, Italy*

Received April 4, 2008

Alzheimer's disease (AD) is becoming a rapidly growing health problem, as it is one of the main causes of dementia in the elderly. Interestingly, copper(II) (together with zinc and iron) ions are accumulated in amyloid deposits, suggesting that metal binding to Aβ could be involved in AD pathogenesis. In Aβ, the metal binding is believed to occur within the N-terminal region encompassing the amino acid residues 1−16. In this work, potentiometric, spectroscopic (UV−vis, circular dichroism, and electron paramagnetic resonance), and electrospray ionization mass spectrometry (ESI-MS) approaches were used to investigate the copper(II) coordination features of a new polyethylene glycol (PEG)-conjugated Aβ peptide fragment encompassing the 1−16 amino acid residues of the N-terminal region (Aβ(1−16)PEG). The high water solubility of the resulting metal complexes allowed us to obtain a complete complex speciation at different metal-to-ligand ratios ranging from 1:1 to 4:1. Potentiometric and ESI-MS data indicate that Aβ(1−16)PEG is able to bind up to four copper(II) ions. Furthermore, in order to establish the coordination environment at each metal binding site, a series of shorter peptide fragments of Aβ, namely, Aβ(1−4), Aβ(1−6), AcAβ(1−6), and AcAβ(8−16)Y10A, were synthesized, each encompassing a potential copper(II) binding site. The complexation properties of these shorter peptides were also comparatively investigated by using the same experimental approach.

## Introduction

In order to be functionally active, a protein has to acquire a unique 3D conformation via a folding, which is originated by the primary amino acid sequence and the cellular environment.[1] A small error in the folding process results in a misfolded structure, which can sometimes be lethal.[2,3] Protein misfolding is believed to be the primary cause of Alzheimer's disease (AD), Parkinson's disease (PD), Huntington's disease (HD), Creutzfeldt−Jakob disease (CJD), and many other degenerative and neurodegenerative disorders,[4] called conformational diseases.[5] The most common feature of all of the neurodegenerative disorders is the occurrence of brain lesions, formed by the intra- or extracellular accumulation of misfolded, aggregated, and ubiquitinated proteins.[6,7] For AD, PD, and CJD, a few cases are familial or inherited, but the remainder are sporadic in nature. Alzheimer's disease is the most common form of cerebral degeneration leading to dementia. The key neuropathological features of AD are the extracellular deposition of Aβ and

* Author to whom correspondence should be addressed. Tel.: +39 095 7385070 (E.R.); +36 52 512900/22303 (I.S.). Fax: +39 095 337678 (E.R.); +36 52 489667 (I.S.). E-mail: erizzarelli@dipchiunict.it (E.R.); sovago@delfin.unideb.hu (I.S.).
† University of Catania.
‡ University of Debrecen.
§ CNR Institute of Biostructures and Bioimaging.

(1) Anfisen, C. B. *Science* **1973**, *181*, 223–230.
(2) Ellis, R. J.; Pinheiro, T. J. *Nature* **2002**, *416*, 483–484.
(3) Kelly, J. W. *Curr. Opin. Struct. Biol.* **1998**, *8*, 101–106.
(4) Dobson, C. M. *Trends Biochem. Sci.* **1999**, *24*, 329–332.
(5) Carrell, R. V.; Lomas, D. A. *Lancet* **1997**, *350*, 134–138.
(6) Berke, S. J. S.; Paulson, H. L. *Curr. Opin. Genet. Dev.* **2003**, *13*, 253–261.
(7) Soto, C. *Nature Rev. Neurosci.* **2003**, *4*, 49–60.

10.1021/ic8006052 CCC: $40.75 © 2008 American Chemical Society
Published on Web 09/23/2008

neurofibrillar tangles in the brain.[8] A central process of A$\beta$ is the cleavage of 39−42 amino acid peptides[9,10] from an otherwise normal membrane protein.[11] A$\beta$ forms amyloid fibrils that are insoluble under physiological conditions.[12] The aggregation of A$\beta$ into cytotoxic amyloid fibers or protofibrils may be a factor in AD-related neuronal apoptosis.[13−15]

Several studies have been focused on the A$\beta$ transition from a monomeric random coil conformation to an aggregated $\beta$-sheet secondary structure. It has been shown that amyloid aggregation may have different origins including primary sequences,[16] peptide concentration,[17] pH,[18] membrane lipids,[19,20] protein complexation,[21] glycation,[22] and transition metal ions.[23−27] Proton-induced X-ray emission studies have revealed elevated levels of $Cu^{2+}$ and $Zn^{2+}$ within the amyloid plaques.[28,29] More recently, a "metallomic map" has been obtained in A$\beta$ amyloid plaques by means of noninvasive and nondestructive analytical tools coupled with laser capture microdissection.[30] Synchrotron-based infrared and X-ray imaging showed a strong spatial correlation between elevated $\beta$-sheet content in A$\beta$ plaques and accumulated Cu and Zn ions, thus emphasizing an association of metal ions with amyloid formation in AD.[31] Recent data also indicate that transition metal ion dyshomeostasis in the brain is closely associated with AD: (i) endogenous synaptic zinc contributes to cerebral amyloid deposition in APP2576 transgenic mice;[32] (ii) trace amounts of copper in water induce A$\beta$ amyloid plaques and learning deficits in an AD rabbit model.[33] However, both dietary Cu exposure and endogenous Cu elevation reduce the A$\beta$ amyloid burden *in vivo*[34,35] and inhibit the aggregation of A$\beta$ peptide 1−42 *in vitro*.[36] Like copper, the zinc appears to have a dual effect on A$\beta$ activity, also showing a protective role against the toxicity of the amyloid peptide.[37] The view outlined above has been further complicated by findings indicating that the $\beta$-amyloid accumulation in AD transgenic mice is markedly and rapidly inhibited by treatment with clioquinol, a copper−zinc chelator.[38,39] A recent paper stresses the usefulness of clioquinol as a "metal−protein attenuation compound" for treating AD, showing at the same time that $Cu^{2+}$ and $Zn^{2+}$ but not $Fe^{3+}$ render the amyloid $\beta$-peptide, A$\beta$(1−40), nonfibrillogenic in nature.[40] All of these data suggest an intricate role for copper(II) and zinc(II) in AD metallobiology. To understand whether particular features in the coordination environments of metal ions might modulate amyloid assembly morphology, with important consequences for cellular toxicity, the binding sites, the conformational changes, and affinity constants of $Cu^{2+}$ and $Zn^{2+}$ complexes with A$\beta$ or peptide fragments thereof have been investigated.[41] Similarly to the above-described biological scenario, conflicting chemical and biophysical results have been reported: different coordination modes, stability constant values, and metal-assisted polypeptide secondary structure changes have been proposed.[42−51]

The 1−16 residue domain is generally considered the binding region for the copper(II) ion in A$\beta$(1−42), but only


(8) Selkoe, D. J. *Nature* **1999**, *399*, 23–31.
(9) Glenner, G. G.; Wong, C. W. *Biochem. Biophys. Res. Commun.* **1984**, *122*, 1131–1135.
(10) Masters, C. L.; Simms, G.; Weinman, N. A.; Multhaup, G.; McDonald, B. L.; Beyreuther, K. *Proc. Natl. Acad. Sci. U.S.A.* **1985**, *82*, 4245–4249.
(11) Kang, J.; Lemaire, H. G.; Unterbeck, A.; Salbaum, J. M.; Masters, C. L.; Grzeschik, K. H.; Multhaup, G.; Beyreuther, K.; Muller-Hill, B. *Nature* **1987**, *325*, 733–736.
(12) Inoue, S.; Kuroiwa, M.; Kisilevski, R. *Brain Res. Rev.* **1999**, *29*, 218–231.
(13) Pike, C. J.; Burdick, D.; Walencewicz, A. J.; Glabe, C. G.; Cotman, C. W. *J. Neurosci.* **1993**, *13*, 1676–1687.
(14) Yankner, B. A. *Neuron* **1996**, *16*, 921–932.
(15) Walsh, D. M.; Hartley, D. M.; Kusumoto, Y.; Fezoni, Y.; Condron, M. M.; Lomakin, A.; Benedek, G. B.; Selkoe, D. J.; Teplow, D. B. *J. Biol. Chem.* **1999**, *274*, 25945–25952.
(16) Fraser, P. E.; Nguyen, J. T.; Surewicz, W. K.; Selkoe, D. J.; Podlisny, M. B.; Kirshner, D. A. *Biochemistry* **1992**, *31*, 10716–10723.
(17) Burdick, D.; Soreghan, B.; Kwon, M.; Kosmoski, J.; Knamer, M.; Henshen, A.; Yates, J.; Cotamn, C.; Glabe, C. *J. Biol. Chem.* **1992**, *267*, 546–554.
(18) Fraser, P. E.; Nguyen, J. T.; Surewicz, W. K.; Kirshner, D. A. *Biophys. J.* **1991**, *60*, 1190–1201.
(19) Yip, C. M.; Darabie, A. A.; McLaurin, J. *J. Mol. Biol.* **2002**, *318*, 97–107.
(20) Ambroggio, E. E.; Kim, D. H.; Separovic, F.; Barrow, C. J.; Barnham, K. J.; Bagatolli, L. A.; Fedelio, G. D. *Biophys. J.* **2005**, *88*, 2706–2713.
(21) Wisniewski, T.; Frangione, B. *Neurosci. Lett.* **1992**, *135*, 235–238.
(22) Vitek, M. P.; Bhattacharia, K.; Glendening, J. M.; Stopa, E.; Vlassara, H.; Bucala, R.; Manogue, K.; Cerami, A. *Proc. Natl. Acad. Sci. U.S.A.* **1994**, *91*, 4766–4770.
(23) Bush, A. I.; Pettingell, W. H.; Multhaup, G.; de Paradis, M.; Vonsattel, J. P.; Gusella, J. F.; Beyreuther, K.; Masters, C. L.; Tanzi, R. E. *Science* **1994**, *265*, 1464–1467.
(24) Atwood, C. S.; Moir, R. D.; Huang, X.; Scarpa, R. C.; Bacarra, N. M.; Romano, D. M.; Harthorn, M. A.; Tanzi, R. E.; Bush, A. I. *J. Biol. Chem.* **1998**, *273*, 12817–12826.
(25) Bush, A. I. *Trends Neurosci.* **2003**, *26*, 207–214.
(26) Maynard, C. J.; Bush, A. I.; Masters, C. L.; Cappai, R.; Li, Q.-X. *Int. J. Exp. Path.* **2005**, *86*, 147–159.
(27) White, A. R.; Barnham, K. J.; Bush, A. I. *Expert Rev. Neurother.* **2006**, *6*, 711–722.
(28) Danscher, G.; Jensen, K. B.; Frederickson, C. J.; Kemp, K.; Andreasen, A.; Juhl, S.; Stoltenberg, M.; Ravid, R. *J. Neurosci. Methods* **1997**, *76*, 53–59.
(29) Lovell, M. A.; Robertson, J. D.; Teesdale, W. J.; Markesbery, W. R. *J. Neurol. Sci.* **1998**, *158*, 47–52.
(30) Liu, G.; Huang, W.; Moir, R. D.; Vanderburg, C. R.; Lai, B.; Peng, Z.; Tanzi, R. E.; Rogers, J. T.; Huang, H. *J. Struct. Biol.* **2006**, *155*, 45–51.
(31) Miller, L. M.; Wang, Q.; Telivala, T. P.; Smith, R. J.; Lanzirotti, A.; Miklossy, J. *J. Struct. Biol.* **2006**, *155*, 30–37.
(32) Lee, J. Y.; Cole, T. B.; Palmiter, R. D.; Suh, S. W.; Koh, J. Y. *Proc. Natl. Acad. Sci. U.S.A.* **2002**, *99*, 7705–7710.
(33) Sparks, D. L.; Schreurs, B. G. *Proc. Natl. Acad. Sci. U.S.A.* **2003**, *100*, 11065–11069.
(34) Bayer, T. A.; Schafer, S.; Simons, S.; Kemmling, A.; Kamer, T.; Tepest, R.; Eckert, A.; Schussel, K.; Eikenberg, O.; Sturchler-Pierrat, C.; Abramowski, D.; Staufenbiel, M.; Multhaup, G. *Proc. Natl. Acad. Sci. U.S.A.* **2003**, *100*, 14187–14192.
(35) Phinney, A. L.; Drisaldi, B.; Schmidt, S. D.; Lugowski, S.; Coronado, V.; Liang, Y.; Horne, P.; Yang, J.; Sekoulidis, J.; Coomaraswamy, J.; Chishti, M. A.; Cox, D. W.; Mathews, P. M.; Nixon, R. A.; Carlson, G. A.; St George-Hyslop, P.; Westaway, D. *Proc. Natl. Acad. Sci. U.S.A.* **2003**, *100*, 14193–14198.
(36) Zou, J.; Kajita, K.; Sugimoto, N. *Angew. Chem., Int. Ed.* **2001**, *40*, 2274–2277.
(37) Cuajungco, M. P.; Faget, K. Y. *Brain Res. Rev.* **2003**, *41*, 44–56.
(38) Cherny, R. A.; Atwood, C. S.; Xilinas, M. E.; Gray, D. N.; Jones, W. D.; McLean, C. A.; Barnham, K. J.; Volitakis, I.; Fraser, F. W.; Kim, Y.-S.; Huang, X.; Goldstein, L. E.; Moir, R. D.; Lim, J. T.; Beyreuther, K.; Zheng, H.; Tanzi, R. E.; Masters, C. L.; Bush, A. I. *Neuron* **2001**, *30*, 665–676.
(39) Finefrock, A. E.; Bush, A. I.; Doraiswamy, P. M. *J. Am. Geriatr. Soc.* **2003**, *51*, 1143–1148.
(40) Raman, B.; Ban, T.; Yamaguchi, K.; Sakai, M.; Kawai, T.; Naiki, H.; Goto, Y. *J. Biol. Chem.* **2005**, *280*, 16157–16162.
(41) Gaggelli, E.; Kozlowski, H.; Valensin, D.; Valensin, G. *Chem. Rev.* **2006**, *106*, 1995–2044.

little potentiometric data have been reported, and all of the results were obtained from experiments carried out at a 1:1 metal-to-peptide ratio, also for a number of peptide fragments of Aβ(1−16).[52−55] Other studies have highlighted the fact that the Aβ can host three to four copper ions per peptide molecule,[24,48] but the precipitate formation did not allow the investigation of the formation of dinuclear or trinuclear species, using potentiometry, and unambiguous assignment of the related metal ions' coordination environment.[41]

It is known that the conjugation with the polyethylene glycol (PEG) moiety enhances the solubility of certain hydrophobic peptides including the Aβ(10−35).[56,57] Thus, a new Aβ(1−16) conjugate, bearing a PEG moiety at the C-terminus, Aβ(1−16)PEG, was synthesized, allowing the metal complex speciation at different metal-to-ligand ratios to be obtained. Both potentiometric and spectroscopic [UV−vis, circular dichroism (CD), and electron paramagnetic resonance (EPR)] studies were carried out in aqueous solution. Furthermore, in order to elucidate the structure of the metal ion complexes formed in the Aβ(1−16) region at various metal-to-ligand ratios, we resort to a comparative study by investigating a series of shorter and single-point mutated peptide analogues. Thus, the wild-type peptide Aβ(1−16); its mutant Aβ(1−16)Y10A; and the Aβ(1−4), Aβ(1−6), Ac-Aβ(1−6), and Ac-Aβ(8−16)Y10A peptide fragments were also studied to assess the involvement of the amino N-terminus, the carboxylate group of different Asp and Glu residues, as well as the different histidine imidazoles and the tyrosine OH group in the binding to copper(II).


(42) Smith, D. P.; Smith, D. G.; Curtain, C. C.; Boas, J. F.; Pilbrow, J. R.; Ciccotosto, G. D.; Lau, T.-L.; Tew, D. J.; Perez, K.; Wade, J. D.; Bush, A. I.; Drew, S. C.; Separovic, F.; Masters, C. L.; Cappai, R.; Barnham, K. J. *J. Biol. Chem.* **2006**, *281*, 15145–15154.

(43) Karr, J. W.; Akintoye, H.; Kaupp, L. J.; Szalai, V. A. *Biochemistry* **2005**, *44*, 5478–5487.

(44) Kozin, S. A.; Zirah, S.; Rebuffat, S.; Hui Bon Hoa, G.; Debey, P. *Biochem. Biophys. Res. Commun.* **2001**, *285*, 959–964.

(45) Zirah, S.; Kozin, S. A.; Mazur, A. K.; Blond, A.; Cheminant, M.; Ségalas-Milazzo, I.; Debey, P.; Rebuffat, S. *J. Biol. Chem.* **2006**, *281*, 2151–2161.

(46) Curtain, C. C.; Ali, F.; Volitakis, I.; Cherny, R. A.; Norton, R. S.; Beyreuther, K.; Barrow, C. J.; Masters, C. L.; Bush, A. I.; Barnham, K. J. *J. Biol. Chem.* **2001**, *276*, 20466–20473.

(47) Huang, X.; Atwood, C. S.; Hartshorn, M. A.; Vonsattel, J. P.; Tanzi, R. E.; Bush, A. I. *J. Biol. Chem.* **1997**, *272*, 26464–26470.

(48) Atwood, C. S.; Scarpa, R. C.; Huang, X.; Moir, R. D.; Jones, W. D.; Fairlie, D. P.; Tanzi, R. E.; Bush, A. I. *J. Neurochem.* **2000**, *75*, 1219–1233.

(49) Miura, T.; Suzuki, K.; Kohata, N.; Takeuchi, H. *Biochemistry* **2000**, *39*, 7024–7031.

(50) Ma, Q.-F.; Hu, J.; Wu, W.-H.; Liu, H.-D.; Fu, Y.; Wu, Y.-W.; Lei, P.; Zhao, Y.-F.; Li, Y.-M. *Biopolymers* **2006**, *83*, 20–31.

(51) Syme, C. D.; Nadal, R. C.; Rigby, S. E. J.; Viles, J. H. *J. Biol. Chem.* **2004**, *279*, 18169–18177.

(52) Kowalik-Jankowska, T.; Ruta-Dolejsz, M.; Wisniewska, K.; Lankiewicz, L.; Kozlowski, H. *J. Chem. Soc., Dalton Trans.* **2000**, *4511*, 4519.

(53) Kowalik-Jankowska, T.; Ruta-Dolejsz, M.; Wisniewska, K.; Lankiewicz, L. *J. Inorg. Biochem.* **2001**, *86*, 535–545.

(54) Kowalik-Jankowska, T.; Ruta-Dolejsz, M.; Wisniewska, K.; Lankiewicz, L. *J. Inorg. Biochem.* **2002**, *92*, 1–10.

(55) Kowalik-Jankowska, T.; Ruta-Dolejsz, M.; Wisniewska, K.; Lankiewicz, L. *J. Inorg. Biochem.* **2003**, *95*, 270–282.

(56) Burkoth, T. S.; Benzinger, T. L. S.; Jones, D. N. M.; Hallenga, K.; Meredith, S. C.; Lynn, D. G. *J. Am. Chem. Soc.* **1998**, *120*, 7655–7656.

(57) Burkoth, T. S.; Benzinger, T. L. S.; Urban, V.; Gregory, D. M.; Thiyagarajan, P.; Botto, R. E.; Meredith, S. C.; Lynn, D. G. *J. Am. Chem. Soc.* **2000**, *122*, 7883–7889.


## Experimental Section

**General.** All N-fluorenylmethoxycarbonyl (Fmoc)-protected amino acids, 2-(1-H-benzotriazole-1-yl)-1,1,3,3-tetramethyluronium tatrafluoroborate (TBTU), O-(N-Fmoc-2-aminoethyl)-O′-(2-carboxyethyl)-undecaethyleneglycol (PEG), and NovaSyn TGR resin were obtained from Novabiochem (Switzerland); Fmoc PAL-PEG resin, N,N-diisopropyl-ethylamine (DIEA), N-[(dimethylamino)-1H-1,2,3-triazolo[4,5-b]pyridine-1-ylmethylene]-N-methylmethanaminium hexafluorophosphate N-oxide (HATU), and a 20% piperidine−N,N-dimethylformamide (DMF) solution were obtained from Applied Biosystems. N-hydroxybenzotriazole (HOBt), triisopropylsilane (TIS), and trifluoroacetic acid (TFA) were purchased from Sigma/Aldrich. DMF (peptide-synthesis-grade) was obtained from Labscan Analytical Sciences. All other chemicals were of the highest available grade and were used without further purification.

Preparative reversed-phase high-performance liquid chromatography (RP-HPLC) was carried out using a Varian PrepStar 200 model SD-1 chromatography system equipped with a Prostar photodiode array detector with detection at 222 nm. Purification was carried out eluting with solvents A (0.1% TFA in water) and B (0.1% TFA in acetonitrile) on a Vydac $C_{18}$ 250 × 22 mm (300 Å pore size, 10−15 μm particle size) column, at a flow rate of 10 mL/min. Analytical RP-HPLC analyses were performed using a Waters 1525 instrument equipped with a Waters 2996 photodiode array detector with detection at 222 nm. The peptide samples were analyzed using gradient elution with solvents A and B on a Vydac $C_{18}$ 250 × 4.6 mm (300 Å pore size, 5 μm particle size), run at a flow rate of 1 mL/min.

**Peptide Synthesis and Purification.** The Aβ(1−16), the Aβ(1−16)PEG, and the Aβ(1−16)Y10A peptides were assembled by standard solid-phase−peptide synthesis on a Pioneer Peptide Synthesizer. All of the amino acid residues were introduced according to the HATU/DIEA activation method for Fmoc chemistry on Fmoc PAL-PEG resin (substitution 0.18 mmol/g). All of the coupling reactions were carried out under a 4-fold excess of amino acid at every cycle. Fmoc deprotection was achieved at every cycle with 20% piperidine solution in DMF.

The Aβ(1−4), the Aβ(1−6), the Ac-Aβ(1−6), and the Ac-Aβ(8−16)Y10A peptides were synthesized by using microwave-assisted solid-phase−peptide synthesis technology on a Liberty Peptide Synthesizer. Amino acid derivatives were introduced according to the TBTU/HOBt/DIEA method on NovaSyn TGR resin (substitution 0.18 mmol/g) following the procedure depicted in Scheme 1.

All of the coupling reactions were carried out under a 4-fold excess of amino acid at every cycle. The following instrumental conditions were used for each coupling cycle: microwave power, 25 W; reaction temperature, 75 °C; coupling time, 300 s. Fmoc deprotection was achieved at every cycle with a 20% piperidine solution in DMF, using the instrumental conditions: microwave power, 25 W; reaction temperature, 75 °C; deprotection time, 180 s. N-terminal acetilation of the Ac-Aβ(1−6) and the Ac-Aβ(8−16)Y10A was performed by treating the fully assembled and protected peptide resins (after removal of the N-terminal Fmoc group) with a solution containing acetic anhydride (6% v/v) and DIEA (5% v/v) in DMF.

The peptides were cleaved from their respective resins and simultaneously deprotected by treatment with a mixture of TFA/TIS/$H_2O$ (95/2.5/2.5 v/v) for 2 h at room temperature. Each solution containing the free peptide was separated from the resin by filtration and concentrated *in vacuo* at 30 °C. All peptides were precipitated with cold freshly distilled diethyl ether. The precipitate was then

**Scheme 1.** General Scheme of a Standard Solid Phase Peptide Synthesis

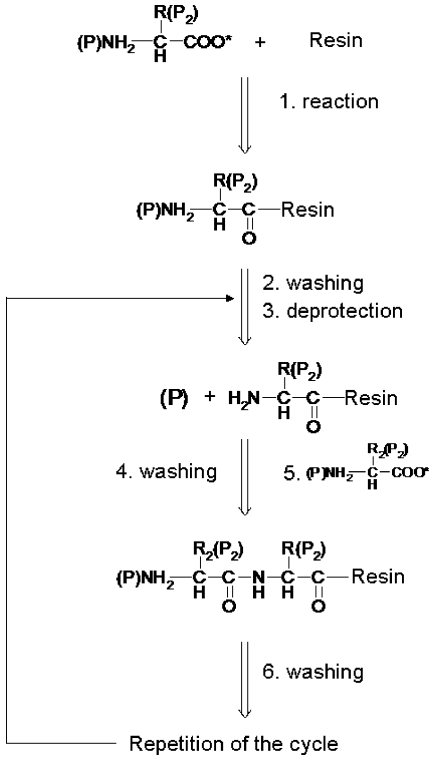


filtered, dried under a vacuum, redissolved in water, and lyophilized. The crude peptides were purified by preparative RP-HPLC, as described below.

**AspAlaGluPheNH$_2$ [A$\beta$(1−4)].** The preparative RP-HPLC process: from 0 to 5 min, isocratic elution in 100% of A; then, a linear gradient from 0% to 18% B for 10 min; finally, isocratic elution in 18% B from 15 to 25 min [$R_t$ = 22.9 min]. The analytical RP-HPLC process: from 0 to 5 min, isocratic elution in 100% A; then, a linear gradient from 0 to 18% B for 10 min; finally, isocratic elution in 18% B from 15 to 20 min [$R_t$ = 18 min]. ESI-MS observed *m*/*z*: $(M + H)^+$ 480.4, $(M + Na)^+$ 502.3. Calculated for $C_{21}H_{29}N_5O_8$ = 479.2.

**AspAlaGluPheArgHisNH$_2$ [A$\beta$(1−6)].** The preparative RP-HPLC process: from 0 to 5 min, isocratic elution in 100% of A; then, a linear gradient from 0% to 14% B for 10 min; finally, isocratic elution in 14% B from 15 to 25 min [$R_t$ = 23.0 min]. The analytical RP-HPLC process: from 0 to 5 min, isocratic elution in 100% A; then, a linear gradient from 0 to 14% B for 10 min; finally, isocratic elution in 14% B from 15 to 20 min [$R_t$ = 19.3 min]. ESI-MS observed *m*/*z*: $(M + H)^+$ 773.5, $(M + 2H)^{2+}$ 387.3. Calculated for $C_{33}H_{48}N_{12}O_{10}$ = 772.4.

**AcAspAlaGluPheArgHisNH$_2$ [Ac-A$\beta$(1−6)].** The analytical RP-HPLC process: from 0 to 5 min, isocratic elution in 100% A; then, a linear gradient from 0 to 30% B for 25 min; finally, isocratic elution in 30% B from 30 to 35 min [$R_t$ = 20.5 min]. ESI-MS observed *m*/*z*: $(M + H)^+$ 815.5, $(M + 2H)^{2+}$ 408.3 Calculated for $C_{35}H_{50}N_{12}O_{11}$ = 814.4.

**AcSerGlyAlaGluValHisHisGlnLysNH$_2$ [Ac-A$\beta$(8−16)Y10A].** The preparative RP-HPLC process: from 0 to 5 min, isocratic elution in 100% of A; then, a linear gradient from 0% to 17% B for 10 min; finally, isocratic elution in 17% B from 15 to 25 min [$R_t$ = 19.9 min]. The analytical RP-HPLC process: from 0 to 5 min, isocratic elution in 100% A; then, a linear gradient from 0 to 17% B for 10 min; finally, isocratic elution in 17% B from 15 to 20 min [$R_t$ = 15.4 min]. ESI-MS observed *m*/*z*: $(M + H)^+$ 1033.5, $(M + 2H)^{2+}$ 517.3, $(M + 3H)^{3+}$ 345.3. Calculated for $C_{43}H_{68}N_{16}O_{14}$ = 1032.5.

**AspAlaGluPheArgHisAspSerGlyTyrGluValHisHisGlnLysNH$_2$ [A$\beta$(1−16)].** The preparative RP-HPLC process: from 0 to 5 min, isocratic elution in 5% of B; then, a linear gradient from 5% to 16% B for 25 min; finally, isocratic elution in 16% B from 30 to 40 min [$R_t$ = 34.8 min]. The analytical RP-HPLC process: from 0 to 5 min, isocratic elution in 5% B; then, a linear gradient from 5 to 16% B for 25 min; finally, isocratic elution in 16% B from 30 to 35 min [$R_t$ = 32.8 min]. ESI-MS observed *m*/*z*: $(M + H)^+$ 1954.3, $(M + 2H)^{2+}$ 977.3, $(M + 3H)^{3+}$ 652.1. Calculated for $C_{84}H_{120}N_{28}O_{27}$ = 1952.9.

**AspAlaGluPheArgHisAspSerGlyTyrGluValHisHisGlnLysPEGNH$_2$ [A$\beta$(1−16)PEG].** The preparative RP-HPLC process: from 0 to 8 min, isocratic elution in 5% of B; then, a linear gradient from 5% to 40% B for 25 min; finally, isocratic elution in 40% B from 33 to 40 min [$R_t$ = 28.4 min]. The analytical RP-HPLC process: from 0 to 5 min, isocratic elution in 5% B; then, a linear gradient from 5 to 40% B for 25 min; finally, isocratic elution in 40% B from 30 to 35 min [$R_t$ = 19.3 min]. ESI-MS observed *m*/*z*: $(M + 2H)^{2+}$ 1277.4, $(M + 3H)^{3+}$ 852.1, $(M + 4H)^{4+}$ 639.5. Calculated for $C_{111}H_{173}N_{29}O_{40}$ = 2552.2.

**AspAlaGluPheArgHisAspSerGlyAlaGluValHisHisGlnLysNH$_2$ [A$\beta$(1−16)Y10A].** The preparative RP-HPLC process: from 0 to 5 min, isocratic elution in 5% of B; then, a linear gradient from 5% to 25% B for 30 min; finally, isocratic elution in 25% B from 35 to 40 min [$R_t$ = 26.4 min]. The analytical RP-HPLC process: from 0 to 5 min, isocratic elution in 5% B; then, a linear gradient from 5 to 25% B for 30 min; finally, isocratic elution in 25% B from 35 to 40 min [$R_t$ = 19.4 min]. ESI-MS observed *m*/*z*: $(M + H)^+$ 1861.4, $(M + 2H)^{2+}$ 931.9, $(M + 3H)^{3+}$ 621.5, $(M + 4H)^{4+}$ 466.7. Calculated for $C_{78}H_{116}N_{28}O_{26}$ = 1860.8.

**Potentiometric and Spectroscopic Measurements.** The potentiometric titrations were performed in 3 cm$^3$ samples exploring the concentration range of $1 \times 10^{-3}$ to $4 \times 10^{-3}$ mol dm$^{-3}$ with metal ion-to-ligand ratios between 4:1 and 1:2. During the titration, argon was bubbled through the samples to ensure the absence of oxygen and carbon dioxide and also to stir the solutions. All measurements were carried out at 298 K and at a constant ionic strength of 0.2 mol dm$^{-3}$ KCl. pH measurements were made with a MOLSPIN pH-meter equipped with a 6.0234.100 combined electrode (Metrohm) and a MOL-ACS microburette controlled by a computer. The recorded pH values were converted into hydrogen ion concentration as described elsewhere.[58] Stability constants (log $\beta_{pqr}$ for $M_pH_qL_r$) were calculated by the general computational programs PSEQUAD,[59] SUPERQUAD,[60] and HYPERQUAD.[61]

UV−vis spectra of complexes were recorded on a Hewlett-Packard HP 8453 diode array spectrophotometer in the same concentration range as used for potentiometry. UV−vis spectra of the systems were recorded at different metal ion-to-ligand ratios in a wide pH range, and it made possible the calculation of the molar absorptivities of the individual species. This calculation was performed by the PSEQUAD[59] computer program using the spectra measured at different pH values and the total concentration of all components and the potentimetrically determined stability constants.

(58) Irving, H.; Miles, G.; Malcolm, G.; Pettit, L. D. *Anal. Chim. Acta* **1967**, *38*, 475–488.
(59) Zékány, L.; Nagypál, I. In *Computational Methods for the Determination of Formation Constants*; Leggett, D. J. Ed.; Plenum Press: New York, 1985; pp 291−355.
(60) Gans, P.; Sabatini, A.; Vacca, A. *J. Chem. Soc., Dalton Trans.* **1985**, 1195–1200.
(61) Gans, P.; Sabatini, A.; Vacca, A. *Talanta* **1996**, *43*, 1739–1753.

All of the CD measurements were carried out at 25 °C under a constant flow of nitrogen on a JASCO model J-810 spectropolarimeter. The CD spectra of copper(II) complexes were recorded in the 300−800 nm range, and the spectra of the individual species were calculated with the PSEQUAD program.[59] Far-UV CD measurements were carried out at different pH values, using 1-mm-path-length cuvettes. The CD spectra of the free peptide ligands were recorded in the UV region (190−260 nm), whereas those in the presence of $Cu^{2+}$ were obtained in the wavelength ranges of 190−380. The spectra represent the average of 10 scans. All of the solutions were freshly prepared using deionized water. A Bruker Elexsys E500 CW-EPR spectrometer driven by a PC running the xEpr program under Linux and equipped with a Super-X microwave bridge operating at 9.3−9.5 GHz and a SHQE cavity was used throughout this work. All EPR spectra of frozen solutions of copper(II) complexes were recorded at 150 K by means of a variable-temperature apparatus. Copper(II) complex aqueous solutions [$(1.0-1.3) \times 10^{-3}$ mol $dm^{-3}$] were prepared starting from $^{63}Cu(NO_3)_2$ and the pertinent peptide varying the pH by adding NaOH followed by the addition of a small amount of methanol (not exceeding 10%) to them. Different metal-to-ligand ratios were also explored, ranging from 1:1 to 2:1. The EPR parameters were obtained directly from the experimental spectra obtained at the maximum concentration of the particular species for which well-resolved separations were observed.

**Electrospray Mass Spectrometry (ESI-MS).** ESI-MS spectra were recorded on a Finnigan LCQ Deca XP ion trap using an electrospray ionization (ESI) interface. Peptide solutions were introduced into the ESI source via 100 μm i.d. fused silica, using a 500 μL syringe. The spectra were acquired in the positive ion mode, and the instrumental conditions were as follows: needle voltage, 2.5 kV; flow rate, 3−5 μL/min; source temperature, 250−300 °C; *m*/*z* range, 50−4000; cone potential, 46 V; tube lens offset, 15 V. The metal complex solutions were prepared by dissolving the peptide and $CuSO_4$ ($5 \times 10^{-5}$ mol $dm^{-3}$ in Milli-Q water) at 1:1, 1:2, 1:3, and 1:4 L/Cu(II) ratios and were investigated in the 3−10.5 pH range, adjusting the pH values by adding HCl or NaOH.

Because of the isotopic distribution of elements, molecular species are detected in the mass spectra as clusters of peaks. To simplify their assignments, the *m*/*z* values indicated in the spectra and in the text correspond to the first (lowest-mass) peak of each cluster.

## Results and Discussion

**The Aβ(1−16)PEG Conformational Features and Its Metal Hosting Capability.** The amino acid sequences of the amyloid-β peptide fragments are shown in Scheme 2.

Previous studies on the complexes of amyloid-β peptide, Aβ(1−42), indicated that the primary metal binding sites are located in the N-terminal region of the peptide. As a consequence, the N-terminal hexadecapeptide fragment Aβ(1−16) is a suitable model to study the interaction of transition metal ions with the native peptide molecule.[41] The PEG-peptide conjugate was assembled using an O-(N-Fmoc-2-aminoethyl)-O′-(2-carboxyethyl)-undecaethylene glycol, which allowed us to employ the solid-phase-peptide synthesis strategy to link the PEG moiety at the C-terminus of Aβ(1−16) by means of an amide bond. Both the peptide derivative Aβ(1−16)PEG and its copper(II) complexes are well soluble in a water solution under all of the experimental conditions employed in the present study.

**Scheme 2.** Amino Acid Sequences of the Peptide Fragments of Amyloid-β Polypeptide

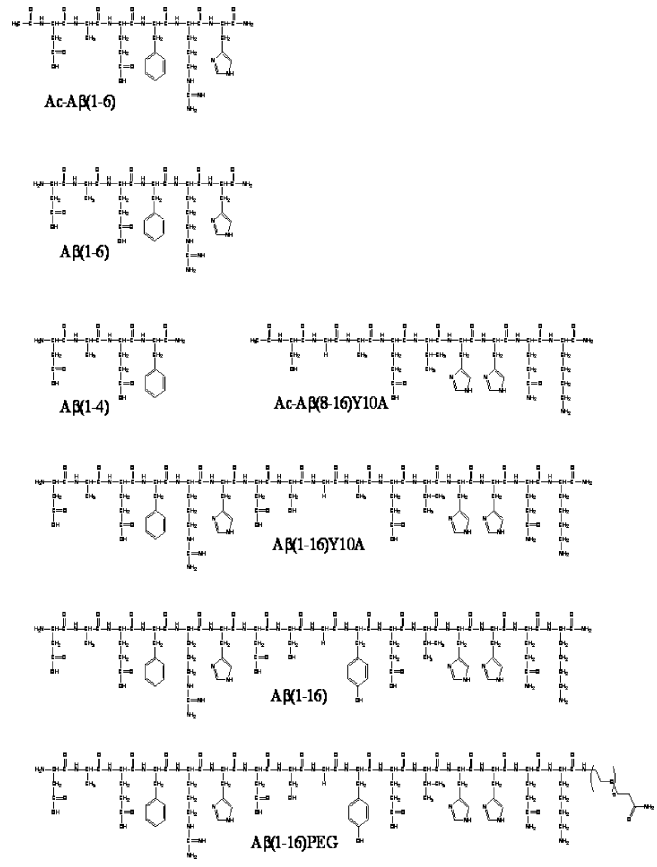


Furthermore, comparative CD experiments on Aβ(1−16)-PEG and wild-type Aβ(1−16) were performed to evaluate any influence of the PEG conjugation on the conformational properties of the peptide fragment (Figure 1).

The CD spectra reveal that both Aβ(1−16)PEG and Aβ(1−16) are in a random-coil conformation in the 4−11 pH range, suggesting that the PEG conjugation does not introduce substantial differences in the conformational properties of the peptide chains at any pH value. In addition, far-UV CD experiments were also carried out in the presence of copper(II). The low concentrations required by these measurements allow us to determine the stoichiometry of copper(II) complexes with Aβ(1−16); the ability of the wild-type peptide to host four copper(II) equivalents is equal to that of the Aβ(1−16)PEG (see Figure 1S in the Supporting Information).

**Protonation Equilibria and Copper(II) Complexes of the N-Terminal Peptide Fragments of Amyloid-β Peptide.** A literature survey[62−65] on the metal binding affinity and selectivity of peptide complexes reveals that both terminal amino and His6 imidazole side chains can be the major binding sites of the N-terminally free hexapeptide

(62) Sigel, H.; Martin, R. B. *Chem. Rev.* **1982**, *82*, 385–426.
(63) Sóvágó, I. In *Biocoordination Chemistry: Metal Complexes of Peptides and Derivatives*; Burger, K. Ed.; Ellis Horwood: Chichester, U.K., 1990; pp 135−184.
(64) Kozlowski, H.; Bal, W.; Dyba, M.; Kowalik-Jankowska, T. *Coord. Chem. Rev.* **1999**, *184*, 319–346.
(65) Sóvágó, I.; Ösz, K. *Dalton Trans.* **2006**, 3841–3854.

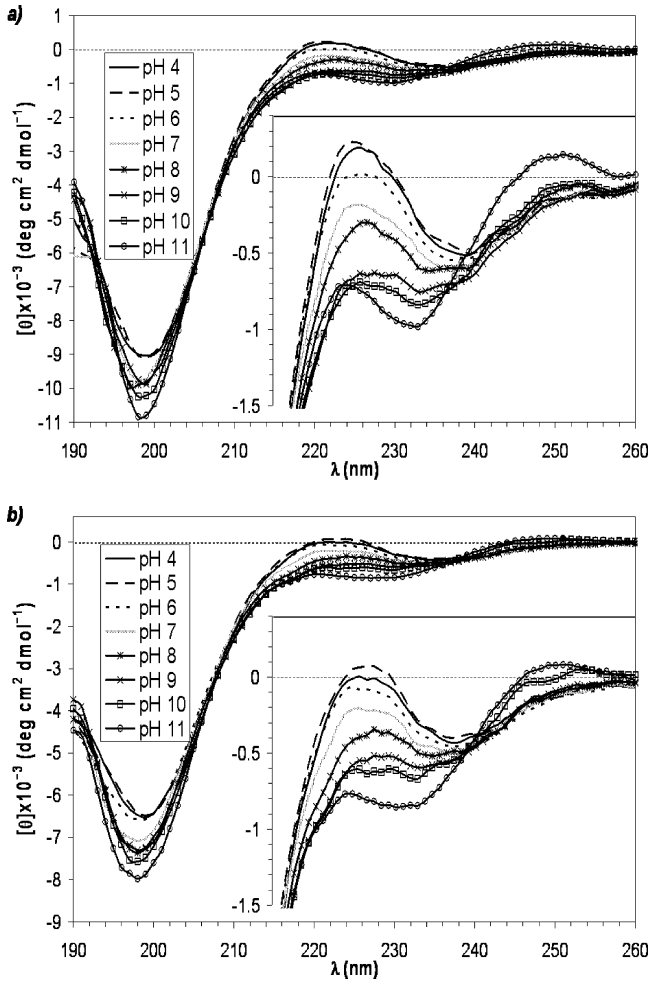


**Figure 1.** Far-UV CD spectra of (a) A$\beta$(1−16)PEG ($c = 1.0 \times 10^{-4}$ mol dm$^{-3}$) and (b) A$\beta$(1−16) ($c = 1.0 \times 10^{-4}$ mol dm$^{-3}$) in $H_2O$ at different pH values. An enlargement of the 216−260 wavelength region is shown in the insets.

A$\beta$(1−6). Therefore, it would be useful to comparatively study the other two peptides, namely, Ac-A$\beta$(1−6) and A$\beta$(1−4), in which only one of the functional groups is available for metal ion coordination. The protonation constants of the three ligands and the stability constants of their copper(II) complexes were determined by potentiometric measurements, and the values are collected in Table 1S (see the Supporting Information).

It is clear from Table 1S that the amino groups show the highest basicities in both N-terminally free peptides, while the p$K$ values of imidazole functions are 6.27 and 6.46 for A$\beta$(1−6) and Ac-A$\beta$(1−6), respectively, and both correspond well to those of other monohistidine ligands. Deprotonation of the carboxylic functions takes place in overlapping processes in a slightly acidic solution, but aspartyl residues are generally more acidic than glutamic acid. The increased acidities of the imidazolium and carboxylic groups of A$\beta$(1−6), as compared to those of the other two ligands, probably come from the double positive charge of $[H_4L]^{2+}$ of A$\beta$(1−6).

The major difference in the complex formation processes of the three ligands is linked to the formation of dinuclear complexes with A$\beta$(1−6), *vide infra*. This observation indicates that both the terminal amino group and the histidyl residue can act as independent metal binding sites and the complex formation processes of A$\beta$(1−6) can be considered as a superimposition of those of Ac-A$\beta$(1−6) and A$\beta$(1−4). Thus, it is better to clarify the complex formation processes of the other two ligands first.

**Copper(II)−A$\beta$(1−4) System.** Stability constants of copper(II) complexes have already been listed in Table 1S, while the spectral parameters of the major species are included in Table 2S (see the Supporting Information).

The p$K$ value of the protonated complex $[CuHL]^+$ is 4.30, supporting the hypothesis that the $\gamma$-carboxylic group of glutamic acid is protonated in this species. The metal binding of $[CuHL]^+$ can be described via either ($NH_2$,CO) or ($NH_2$,$COO^-$) coordination modes. The former is characteristic of simple oligoglycines,[66] while the latter is characteristic for peptides containing N-terminal aspartyl residues,[67] as the A$\beta$(1−4). The stability constant of $[CuHL]^+$ strongly supports the ($NH_2$,$COO^-$) binding mode in which the $\beta$-carboxylate function of Asp1 forms a six-membered chelate with the terminal amino group (the value log $\beta$ = 5.56 and 6.56 were reported for the [CuL] species of GlyGly[66] and AspAla,[67] respectively). The deprotonation of $[CuHL]^+$ is accompanied by a slight red shift of the absorption maximum, suggesting a weak axial interaction of the free glutamyl carboxylate function in the resulting [CuL] complex species. No CD activity can be observed in this pH range, supporting that the amide groups are not involved in metal binding in the species $[CuHL]^+$ and [CuL]. Further deprotonation reactions are, however, accompanied by significant blue shifts of the absorption maximum, supporting the presence of one, two, and three deprotonated amide nitrogens in the species $[CuH_{-1}L]^-$, $[CuH_{-2}L]^{2-}$, and $[CuH_{-3}L]^{3-}$, respectively. The p$K$ values reported for the subsequent deprotonation of the amide functions of tetraglycine are 5.56, 6.91, and 9.18.[66] The comparison of these values with those listed for A$\beta$(1−4) in Table 1S (p$K$($n$/$m$) values) reveals that the enhanced stability of the [CuL] species slightly shifts to higher pH values with the binding of the first amide function, but the other values are quite similar to those of the most common tetrapeptides. CD activity of the complexes was observed above pH 6, and the values reported for $[CuH_{-2}L]^{2-}$ and $[CuH_{-3}L]^{3-}$ in Table 2S are in good agreement with other 3N- and 4N-coordinated copper(II) complexes. As a consequence, it can be unambiguously stated that complex formation processes of A$\beta$(1−4) are quite similar to those of other common tetrapeptides, with the exception of a slight stability enhancement caused by the presence of an N-terminal aspartyl residue.

**Copper(II)−Ac-A$\beta$(1−6) System.** The stability constants obtained for the complexes formed in the copper(II)−Ac-A$\beta$(1−6) system are listed in Table 1S and suggest a speciation similar to that of A$\beta$(1−4) or simple oligopeptides. The species distribution diagram of the system (see Figure 2S

(66) Kállay, C.; Várnagy, K.; Micera, G.; Sanna, D.; Sóvágó, I. *J. Inorg. Biochem.* **2005**, *99*, 1514–1525.
(67) Sóvágó, I.; Sanna, D.; Dessi, A.; Várnagy, K.; Micera, G. *J. Inorg. Biochem.* **1996**, *63*, 99–117.

in the Supporting Information), however, reveals some differences too, suggesting the different binding modes of the two ligands. On one hand, Aβ(1−4) is a more effective metal binder than Ac-Aβ(1−6); for example, about 90% of copper(II) is free in the copper(II)−Ac-Aβ(1−6) system at pH 4, while this value is only 50% for Aβ(1−4). On the other hand, deprotonation and metal ion coordination of the amide functions take place in well-separated reactions for Aβ(1−4), while cooperative deprotonation of the first two amide functions is characteristic for Ac-Aβ(1−6). Similar coordination features have been reported for the copper(II) complexes of peptide fragments of prion proteins, when the blocked N-termini and the histidyl residues are well separated in the peptides.[68−70] The spectroscopic data collected in Table 2S also support this conclusion.

The low concentrations of $[CuHL]^+$ and $[CuH_{-1}L]^-$ rule out the calculation of CD and EPR spectral parameters for these species, but the visible spectra indicate the complexation of copper(II) above pH 4. The CD activity of d−d bands, however, appears only in parallel with the formation of the 3N complex ($[CuH_{-2}L]^{2-}$). The stability constant value of [CuL] indicates the involvement of the imidazole residue and the carboxylate functions of Asp and Glu residues in the form of a macrochelate. This is best reinforced by comparing these data with those of prion fragments. For the monohistidine prion fragments, in which no additional donor sites were available for metal binding, log $\beta \sim 3.6-4.0$ values were reported for the $Cu-N_{im}$ bonded species, and the absorption maxima appeared at 760−770 nm.[70] As a consequence, the values in Table 2S for [CuL] are in agreement with the coordination of the 1N donor atom supported by weak equatorial interaction of the carboxylate function(s). At the same time, the comparison of both equilibrium and spectroscopic data (see $\lambda_{max}$ and EPR values in Table 2S) of $[CuH_{-2}L]^{2-}$and $[CuH_{-3}L]^{3-}$ reveal that the coordination modes of Ac-Aβ(1−6) are the same as those of prion fragments, that is, $(N^-,N^-,N_{im})$ and $(N^-,N^-,N^-,N_{im})$ for $[CuH_{-2}L]^{2-}$ and $[CuH_{-3}L]^{3-}$, respectively.

**Copper(II)−Aβ(1−6) System.** The formation of both mono- and dinuclear complexes represents the most important feature of the coordinating properties of the N-terminally free hexapeptide Aβ(1−6). Previous studies on the copper(II) complexes of some other N-terminal fragments of the amyloid-β peptide suggested the exclusive formation of mononuclear complexes in these systems.[53,55] However, it is important to emphasize that the earlier studies were performed at equimolar concentrations of the metal ion and ligand where mononuclear species predominate. Our studies performed at different metal ion-to-ligand ratios, however, provide an unambiguous proof of the existence of dinuclear species but, at the same time, preclude the formation of bis(ligand) complexes.

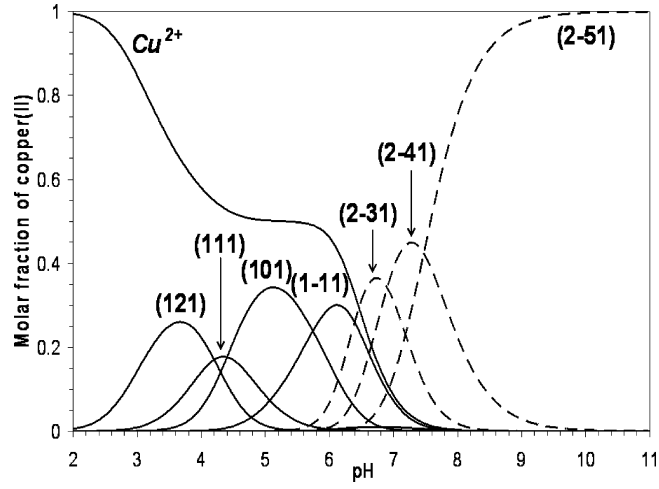


**Figure 2.** Species distribution of the complexes formed in the copper(II)−Aβ(1−6) system ($c_{Cu(II)} = 4 \times 10^{-3}$ mol dm$^{-3}$, $c_L = 2.0 \times 10^{-3}$ mol dm$^{-3}$).

Stability constants of the copper(II) complexes are included in Table 1S, while the corresponding speciation curves at a metal ion-to-ligand ratio of 2:1 are shown in Figure 2.

Taking into account the results obtained for Aβ(1−4) and Ac-Aβ(1−6), it can be stated that there are at least two primary binding sites in Aβ(1−6). The comparison of the stability constants of these ligands clearly indicates that the amino terminus is a more effective anchoring site for metal binding. This suggests that the six-membered chelate with the coordination of the aspartyl amino and carboxylate functions is the common coordination mode of at least three species, $[CuH_2L]^{2+}$, $[CuHL]^+$, and [CuL] in slightly acidic solutions. Both side-chain glutamyl carboxylate and histidyl imidazole functions are protonated in the $[CuH_2L]^{2+}$ species. Taking into account the p$K$ values of these functions, a log $K = 6.91$ can be obtained for the $(NH_2,COO^-)$ binding, which is in good agreement with the stability constants of β-alanine (log $\beta_1 = 6.99 \pm 0.07$ was recommended for $[CuL]^+$ species of β-alanine).[71] Similarly, the species $[CuHL]^+$ can be described by the protonation of the imidazole-N donor atom, and the corresponding stability constant (log $K = 6.89$) supports the exclusive binding of the terminal amino and carboxylate functions. On the other hand, the deprotonation of the imidazolium side chain increases the thermodynamic stability of this coordination mode, supporting the fact that imidazole-N of Aβ(1−6) forms a macrochelate in [CuL]. Since the deprotonation reactions of the complexes largely overlap, the spectral parameters were calculated only for the major species (see Table 2S), and they provide further support for the existence of macrochelates.

The lack of CD activity of d−d bands below pH 5.5 rules out the possibility of amide binding in the [CuL] species, but the transformation of the di- and monoprotonated complexes to the [CuL] species is accompanied by a

(68) Di Natale, G.; Grasso, G.; Impellizzeri, G.; La Mendola, D.; Micera, G.; Mihala, N.; Nagy, Z.; Ösz, K.; Pappalardo, G.; Rigó, V.; Rizzarelli, E.; Sanna, D.; Sóvágó, I. *Inorg. Chem.* **2005**, *44*, 7214–7225.

(69) Grasso, D.; Grasso, G.; Guantieri, V.; Impellizzeri, G.; La Rosa, C.; Milardi, D.; Micera, G.; Ösz, K.; Pappalardo, G.; Rizzarelli, E.; Sanna, D.; Sóvágó, I. *Chem.−Eur. J.* **2006**, *12*, 537–547.

(70) Jószai, V.; Nagy, Z.; Ösz, K.; Sanna, D.; Di Natale, G.; La Mendola, D.; Pappalardo, G.; Rizzarelli, E.; Sóvágó, I. *J. Inorg. Biochem.* **2006**, *100*, 1399–1409.

(71) Sóvágó, I.; Kiss, T.; Gergely, A. *Pure Appl. Chem.* **1993**, *65*, 1029–1080.

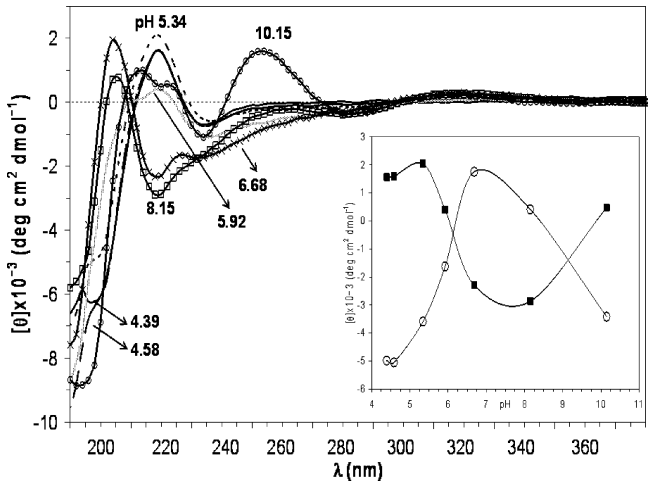


**Figure 3.** Far-UV CD spectra of the copper(II)−A$\beta$(1−6) system ($c_{A\beta(1-6)} = c_{Cu(II)} = 3.3 \times 10^{-5}$ mol dm$^{-3}$) in $H_2O$ at different pH values. Inset: Plots of $[\theta]_{203}$ (open circle) and $[\theta]_{220}$ (closed square) vs pH.

significant blue shift of the absorption maximum in agreement with the increased number of coordinated nitrogen donors in the latter species.[62]

CD spectra provide an unambiguous proof of the existence of Cu−N(amide) bonds in $[CuH_{-1}L]^-$, $[CuH_{-2}L]^{2-}$, and $[CuH_{-3}L]^{3-}$ species.[62] There are two major possibilities for the development of these binding modes: from the N-terminus, as reported for A$\beta$(1−4), or from the histidyl residue, as shown for Ac-A$\beta$(1−6). Both equilibrium and spectroscopic data reveal that the amide binding starts from the N-terminus in the species $[CuH_{-1}L]^-$ and $[CuH_{-2}L]^{2-}$, while a coordination equilibrium exists in the 4N complexes, $[CuH_{-3}L]^{3-}$. In equimolar solutions, $[CuH_{-1}L]^-$ is the predominating complex at physiological pH (see Figure 3S in the Supporting Information), while it is practically missing in the copper(II)−Ac-A$\beta$(1−6) system. Therefore, its coordination mode is best described with the ($NH_2$,$N^-$,$N_{im}$) binding sites in which the ($NH_2$,$N^-$) five-membered chelate is assisted by the macrochelation with the $N_{im}$ donor of the His6 residue. The most convincing proof for the existence of such a macrochelate comes from the EPR spectroscopic parameters (See Table 2S). Indeed, the relatively low $g_{||}$ and $A_{||}$ values support the coordination of 3N donor atoms in a highly distorted environment. Similar data have already been published for the copper(II) complexes of Gly$_n$His peptides, for example, $g_{||} = 2.230$ and $A_{||} = 156$ ($\times 10^{-4}$ cm$^{-1}$) values were reported for the $[CuH_{-1}L]^-$ species of Gly$_5$His containing the same ($NH_2$,$N^-$,$N_{im}$) coordination mode.[72] The far-UV CD spectra of A$\beta$(1−6), in the 6−8 pH range (Figure 3), show that the addition of an equimolar amount of copper(II) causes the appearance of a positive band at 203−205 nm, whereas the initial negative peak at 198 nm disappears. In addition, an inversion of chirality of the band at 218−220 nm can be observed in the same pH range (see inset). These changes match with the formation of the $[CuH_{-1}L]^-$ species, which predominates in the pH range mentioned above, and are indicative of a metal-induced structuring effect of the peptide main chain from a random coil to a $\beta$-turn-like conformation, which can occur only as a consequence of the formation of the macrochelate.

The complex $[CuH_{-3}L]^{3-}$ is a single species above pH 10.0, and its spectral parameters strongly support the existence of a 4N complex. However, its coordination mode can be either ($NH_2$,$N^-$,$N^-$,$N^-$) or ($N^-$,$N^-$,$N^-$,$N_{im}$). UV−vis spectra and EPR parameters (See Table 2S) of the complexes with these binding modes are rather similar to each other, but there are characteristic differences in their CD spectra. CD spectra of the $[CuH_{-3}L]^{3-}$ complex of A$\beta$(1−6) as compared to those of A$\beta$(1−4) and Ac-A$\beta$(1−6) (see Figure 4S in the Supporting Information) reveal that CD extrema of A$\beta$(1−6) complexes can be obtained from the superimposition of the other two systems. It means that coordination isomers of $[CuH_{-3}L]^{3-}$ species exist with the favored ratio for the ($NH_2$,$N^-$,$N^-$,$N^-$) binding mode. This is in agreement with the results of a model calculation in the copper(II)−A$\beta$(1−4)−Ac-A$\beta$(1−6) = 1:1:1 ternary system containing the same binding sites in separated molecules. In the model system, copper(II) ions distribute among the two ligands, but the coordination of the N-terminus ($\sim$ 80%) is favored over the histidyl side chain ($\sim$20%).

Figure 2 reveals that dinuclear complexes are formed only above pH 5.5 in parallel with the involvement of amide functions in metal binding. It is obvious that both chelating sites, the N-terminus and the histidyl side chain, work as independent anchoring sites for metal binding with the subsequent deprotonation and coordination of amide functions. The total number of amide functions in a hexapeptide is, however, only five, and as a consequence, the highest deprotonation state of the complexes is $[Cu_2H_{-5}L]^{3-}$, which is the major species above pH 9. The absorption maximum of the species $[Cu_2H_{-5}L]^{3-}$ appears at 515−520 nm with a molar absorptivity of 175 M$^{-1}$ cm$^{-1}$. The bandwidth is, however, 150 nm for the dinuclear and only 120 nm for the mononuclear species. These values strongly suggest that the $[Cu_2H_{-5}L]^{3-}$ stoichiometry is a superimposition of 4N- and 3N-coordinated copper(II) ions for which the absorption maxima were recorded in the ranges 515−525 and 580−600 nm, respectively. A careful analysis of the CD spectra (see Figure 4S in the Supporting Information) reveals that the coordination geometry of $[Cu_2H_{-5}L]^{3-}$ is not simply a mixture of 3N and 4N complexes, but these binding modes can occur with the involvement of both anchoring groups, that is, ([$NH_2$,$N^-$,$N^-$,$N^-$] + [$N^-$,$N^-$,$N_{im}$]) or ([$NH_2$,$N^-$,$N^-$] + [$N^-$,$N^-$,$N^-$,$N_{im}$]), with a significant preference for the first set of donor atoms. The stoichiometries of the other two dinuclear complexes are $[Cu_2H_{-3}L]^-$ and $[Cu_2H_{-4}L]^{2-}$, containing a total of three and four amide donor functions per ligand, respectively. Taking into account the preferred cooperative deprotonation of two amide functions starting from the histidyl residue, it can be hypothesized that two amide functions mainly come from the histidyl site of the peptide, and the other one or two coordinated amide nitrogens are located close to the N-terminus. The EPR experiments provide further support for dinuclear complex formation. In

(72) Várnagy, K.; Szabó, J.; Sóvágó, I.; Malandrinos, G.; Hadjiliadis, N.; Sanna, D.; Micera, G. *J. Chem. Soc., Dalton Trans.* **2000**, 467–472.

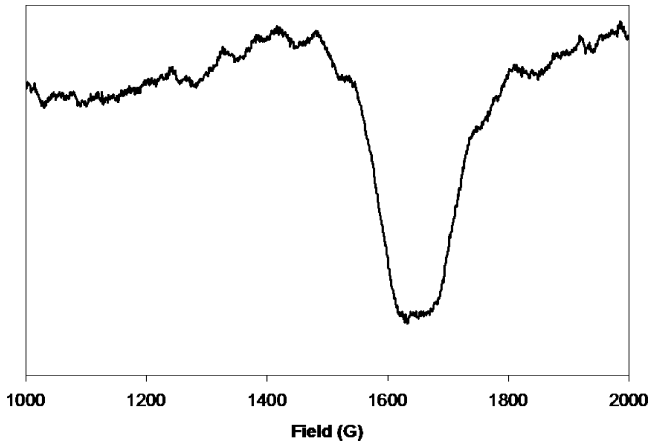


**Figure 4.** Experimental half-field EPR spectrum of the copper(II)−Aβ(1−6) system ($c_{A\beta(1-6)} = 5.0 \times 10^{-3}$ mol dm$^{-3}$, $c_{Cu(II)} = 10.0 \times 10^{-3}$ mol dm$^{-3}$) in frozen solution at pH 7.7.

particular, the significant line broadening of the EPR spectra at $g \sim 2$ and the detection of $\Delta M = 2$ resonances are indicative of a dipolar-type interaction between the metal ions (Figure 4).

ESI-MS experiments, carried out on the copper(II)−Aβ-(1−6) system in the 5−9 pH range, show species stoichiometries in agreement with those found by means of potentiometric investigations (see Table 3S in the Supporting Information).

**Protonation Equilibria and Copper(II) Complexes of Ac-Aβ(8−16)Y10A.** The nonapeptide Ac-Aβ(8−16)Y10A represents the internal part of the amyloid-β peptide containing two neighboring histidyl residues (His13 and His14) as the most effective anchoring sites for metal binding. In the native molecule, a tyrosyl residue is located in position 10, but as will be discussed later, this moiety is not a metal binding site; we used a mutated peptide in which the tyrosine is replaced by an alanine residue to demonstrate this. There are, however, two additional side-chain donor functions, Glu11 and Lys16, which may also take part in acid−base reactions. Protonation constants of the ligand and the stability constants of the copper(II) complexes are included in Table 4S (see the Supporting Information), while Figure 5S (see the Supporting Information) shows the metal ion speciation at different metal ion-to-ligand ratios.

There are four protonation sites in this ligand. Among them, the lysyl amino group is the most basic, while protonation of the two histidyl residues takes place in overlapping processes. The average value for the protonation of the imidazole functions is p$K$ = 6.35, which is very close to other His residues in peptides, for example, to those of Ac-Aβ(1−6) and Aβ(1−6). The acidity of the glutamyl γ-carboxylic function is also in a good agreement with other peptides of glutamic acid.[66]

The 1:1 complexes are present in six different protonation states (from $[CuH_2L]^{3+}$ to $[CuH_{-3}L]^{2-}$), and they are formed in overlapping processes (Figure 5Sa in the Supporting Information). Complex formation starts above pH 4, suggesting that the carboxylate function of the glutamyl residue is deprotonated in the various complexes, while the deprotonation of the noncoordinated lysyl ammonium group takes place only above pH 10 in parallel with the deprotonation of the free ligand. The high number of the different species and the overlapping processes rule out the calculation of the UV−vis and CD spectral parameters of all individual species, but the careful analysis of the pH dependence of these spectra helps to identify the major binding modes. Some parameters of the major species are included in Table 5S (see the Supporting Information), while the pH dependence of UV−vis and CD spectra are reported in Figures 6S and 7S (see the Supporting Information).

The absorption maxima of the copper(II)−Ac-Aβ-(8−16)Y10A system are continuously shifted to the lower wavelengths by increasing pH, but they are above 660 nm below pH 5.5. On the other hand, CD extrema of the d−d bands cannot be detected below pH 5.5, and these data indicate that the $N_{im}$ donor atoms are the exclusive metal binding sites in the protonated complexes $[CuH_2L]^{3+}$ and $[CuHL]^{2+}$. Taking into account the p$K$ values of the ligand, log $K$ = 3.86 can be obtained for the monodentate Cu−$N_{im}$ binding, and it is in good agreement with the values obtained for other histidine-containing peptides.[68−70] In the case of the monoprotonated complex, log $K$ = 5.77 can be obtained supporting the metal ion coordination of both histidyl residues in the form of a macrochelate. It is important to note that the thermodynamic stabilities of other 2 × $N_{im}$ macrochelates are generally between 6 and 7 log units, for example, for HGH sequences.[73−75] Thus, in the case of Ac-Aβ(8−16)Y10A, the histidyl residues (His13 and His14) are too close to each other to form a high-stability species, and the 11-membered macrochelate provides only a rather strained structure.

All spectroscopic parameters (see $\lambda_{max}$ and EPR parameters in Table 5S) indicate that the species from $[CuL]^{+}$ to $[CuH_{-3}L]^{2-}$ contain increasing numbers of coordinated amide nitrogens (1−3 N atoms) by increasing pH. The lack of any spectral changes above pH 10.5 suggests that the last deprotonation belongs to the lysyl ammonium group (see the p$K$(−2/−3) value in Table 4S), and both $[CuH_{-2}L]^{-}$ and $[CuH_{-3}L]^{2-}$ have the same ($N^-$,$N^-$,$N^-$,$N_{im}$) binding mode characteristic of the copper(II) complexes of terminally protected peptides of histidine.[68−70] Spectral parameters in Table 5S strongly support the existence of these coordination modes. Only very small CD and UV−vis spectral changes can be observed in the pH range 6−8. This observation indicates that the species $[CuL]^{+}$ and $[CuH_{-1}L]$ have the same or similar coordination modes. In the case of $[CuH_{-1}L]$, the characteristic 3N complexes with the ($N^-$,$N^-$,$N_{im}$) binding mode can be easily identified around pH 8, while its similarity with $[CuL]^{+}$ can be explained by the existence of coordination isomers. One of the isomers is a 2N complex with the ($N^-$,$N_{im}$) coordination mode, but its concentration is rather low, because the deprotonation of the first two amide groups generally occurs in a cooperative process (e.g., as it

(73) Bóka, B.; Myari, A.; Sóvágó, I.; Hadjiliadis, N. *J. Inorg. Biochem.* **2004**, *98*, 113–122.
(74) Sanna, D.; Micera, G.; Kállay, C.; Rigó, V.; Sóvágó, I. *Dalton Trans.* **2004**, 2702–2707.
(75) Kállay, C.; Várnagy, K.; Malandrinos, G.; Hadjiliadis, N.; Sanna, D.; Sóvágó, I. *Dalton Trans.* **2006**, 4545–4552.

was shown for the copper(II)−Ac-A$\beta$(1−6) system). The other isomer is a 3N complex with the ($N^-$,$N^-$,$N_{im}$) binding mode, and the second imidazole is still protonated in this species below pH 7 ([$CuH_{-1}L$] = [$CuH_{-2}LH$]).

Table 4S and the corresponding speciation curves (Figure 5Sb) reveal that dinuclear species are also formed in the copper(II)−Ac-A$\beta$(8−16)Y10A system (Figure 5Sb); the dinuclear species are present also in equimolar samples, but they predominate only in the presence of an excess of metal ions. This is a difference from previous studies in the literature and can be explained by the fact that the previous works have been performed only in equimolar solutions.[52,54] The most important consequence of this observation is that the nonapeptide Ac-A$\beta$(8−16)Y10A can keep an excess of copper(II) ions in solution both in the physiological pH range and under strongly alkaline conditions. It is also clear from Figure 5S (see the Supporting Information) that the formation of dinuclear complexes is connected to the involvement of amide functions in metal binding, and it occurs only above pH 5. This is an indirect proof of the existence of a $2 \times N_{im}$ macrochelate in the $[CuHL]^{2+}$ species. However, after the deprotonation of the first amide function, the two imidazoles become separate sites for metal binding. The stoichiometries of the dinuclear complexes cover the range from $[Cu_2H_{-1}L]^{2+}$ to $[Cu_2H_{-6}L]^{3-}$, suggesting that two to six amide functions are deprotonated and coordinated in the dinuclear species. The high number of different complexes and the overlap of the deprotonation processes preclude the determination of spectral parameters of all independent species, but the parameters of the final one ($[Cu_2H_{-6}L]^{3-}$) can be easily obtained (see Table 5S). These parameters are similar to those of the corresponding mononuclear complexes, but there are also some minor differences. In the mononuclear species, $[CuH_{-3}L]^{2-}$, His13 is the most probable anchoring site for metal ion coordination, and subsequent amide functions are deprotonated on the N-terminal side of this histidine in the form of (6,5,5)-membered fused chelates. The second copper(II) ion can bind only to His14, and the amide will form a (7,5,5)-membered chelate system toward the C-terminus, which is definitely less stable than the six-membered ones. It is also important to note that in the pH range 6−10 only a broad unresolved EPR signal can be detected in the 2:1 samples of copper(II) and Ac-A$\beta$(8−16)Y10A. However, the absence of a half-field transition signal proves that there is no dipolar interaction between the two copper(II) ions. As a consequence, the formation of an intramolecular imidazolate bridge between the metal ions can be ruled out.[42] Moreover, according to the potentiometric results, ESI-MS measurements of the copper(II)−Ac-A$\beta$(8−16)Y10A system at 1:1, 2:1, and 1:2 metal-to-ligand ratios do not indicate any presence of intermolecular metal imidazolate bridge species under the present experimental conditions (data not shown).

**Protonation Equilibria and Copper(II) Complexes of A$\beta$(1−16), A$\beta$(1−16)Y10A, and A$\beta$(1−16)PEG.** The hexadecapeptide A$\beta$(1−16) and especially its copper(II) complexes have rather low solubility in water, which prevents the complete clarification of the solution equilibrium processes of the system at different metal ion-to-ligand ratios and different pH values. The conjugation of the peptide with PEG, however, results in an enhanced solubility of both the free ligand (A$\beta$(1−16)PEG) and its metal complexes. The p$K$ values of the ligand and the stability constants of the copper(II) complexes are shown in Tables 1 and 2, respectively. The A$\beta$(1−16)PEG has 10 protonation sites, and their assignments are also shown in Table 1. The side-chain amino group of lysine and the phenolic OH of tyrosine

**Table 1.** Protonation Constants (log $\beta_{pqr}$) and pK Values of the A$\beta$(1−16)PEG ($T$ = 298 K, $I$ = 0.2 mol $dm^{-3}$ KCl)

| species | log $\beta_{pqr}$ ($p$ = 0) | p$K$ | site of protonation |
|---|---|---|---|
| $[HL]^{4-}$ | 10.44(1) | 10.44 | Lys-$NH_2$/Tyr-OH |
| $[H_2L]^{3-}$ | 20.22(1) | 9.78 | Tyr-OH/Lys-$NH_2$ |
| $[H_3L]^{2-}$ | 27.91(2) | 7.69 | terminal-$NH_2$ |
| $[H_4L]^{-}$ | 34.64(1) | 6.73 | imidazole of His6, His13 and His14 |
| $[H_5L]$ | 41.03(2) | 6.39 | |
| $[H_6L]^{+}$ | 46.62(4) | 5.59 | |
| $[H_7L]^{2+}$ | 50.83(7) | 4.21 | −COOH of Glu3 and Glu11 |
| $[H_8L]^{3+}$ | 54.73(7) | 3.90 | |
| $[H_9L]^{4+}$ | 57.76(8) | 3.03 | −COOH of Asp1 and Asp7 |
| $[H_{10}L]^{5+}$ | 59.63(9) | 1.87 | |

**Table 2.** Stability Constants (log $\beta_{pqr}$) of the Copper(II) Complexes with A$\beta$(1−16)PEG Peptide ($T$ = 298 K, $I$ = 0.2 mol $dm^{-3}$ KCl)[a]

| mononuclear complexes | | dinuclear complexes (d) | |
|---|---|---|---|
| species | log $\beta_{pqr}$ | species | log $\beta_{pqr}$ |
| $[CuH_7L]^{4+}$ | 54.64(3) | $[Cu_2H_3L]^{2+}$ | 40.16(3) |
| $[CuH_6L]^{3+}$ | 51.01(9) | $[Cu_2H_2L]^{+}$ | 35.22(2) |
| $[CuH_5L]^{2+}$ | 46.70(3) | $[Cu_2HL]$ | 29.43(2) |
| $[CuH_4L]^{+}$ | 42.02(3) | $[Cu_2L]^{-}$ | 22.50(7) |
| $[CuH_3L]$ | 36.77(2) | $[Cu_2H_{-1}L]^{2-}$ | 15.30(4) |
| $[CuH_2L]^{-}$ | 30.46(3) | $[Cu_2H_{-2}L]^{3-}$ | 6.80(9) |
| $[CuHL]^{2-}$ | 22.91(4) | $[Cu_2H_{-3}L]^{4-}$ | −2.28(9) |
| $[CuL]^{3-}$ | 14.49(5) | $[Cu_2H_{-4}L]^{5-}$ | −11.78(10) |
| $[CuH_{-1}L]^{4-}$ | 5.35(6) | $[Cu_2H_{-5}L]^{6-}$ | −22.45(10) |
| $[CuH_{-2}L]^{5-}$ | −4.15(8) | $[Cu_2H_{-6}L]^{7-}$ | −33.59(11) |
| $[CuH_{-3}L]^{6-}$ | −14.79(11) | p$K$(3d/2d) | 4.94 |
| p$K$(7/6) | 3.63 | p$K$(2d/1d) | 5.79 |
| p$K$(6/5) | 4.31 | p$K$(1d/0d) | 6.93 |
| p$K$(5/4) | 4.68 | p$K$(0d/−1d) | 7.20 |
| p$K$(4/3) | 5.25 | p$K$(−1d/−2d) | 8.50 |
| p$K$(3/2) | 6.31 | p$K$(−2d/−3d) | 9.08 |
| p$K$(2/1) | 7.55 | p$K$(−3d/−4d) | 9.50 |
| p$K$(1/0) | 8.42 | p$K$(−4d/−5d) | 10.67 |
| p$K$(0/−1) | 9.14 | p$K$(−5d/−6d) | 11.14 |
| p$K$(−1/−2) | 9.50 | | |
| p$K$(−2/−3) | 10.64 | | |

| trinuclear complexes (tr) | | tetranuclear complexes (te) | |
|---|---|---|---|
| species | log $\beta_{pqr}$ | species | log $\beta_{pqr}$ |
| $[Cu_3H_{-1}L]$ | 19.00(2) | $[Cu_4H_{-4}L]^{-}$ | 2.59(6) |
| $[Cu_3H_{-2}L]^{-}$ | 13.80(9) | $[Cu_4H_{-5}L]^{2-}$ | −4.05(4) |
| $[Cu_3H_{-3}L]^{2-}$ | 6.79(3) | $[Cu_4H_{-6}L]^{3-}$ | −12.16(6) |
| $[Cu_3H_{-4}L]^{3-}$ | −0.70(5) | $[Cu_4H_{-7}L]^{4-}$ | −20.45(5) |
| $[Cu_3H_{-5}L]^{4-}$ | −9.29(6) | $[Cu_4H_{-8}L]^{5-}$ | −29.49(5) |
| $[Cu_3H_{-6}L]^{5-}$ | −18.39(9) | $[Cu_4H_{-9}L]^{6-}$ | −39.17(7) |
| $[Cu_3H_{-7}L]^{6-}$ | −28.09(9) | $[Cu_4H_{-10}L]^{7-}$ | −49.60(9) |
| $[Cu_3H_{-8}L]^{7-}$ | −39.14(10) | $[Cu_4H_{-11}L]^{8-}$ | −60.14(9) |
| $[Cu_3H_{-9}L]^{8-}$ | −50.77(11) | $[Cu_4H_{-12}L]^{9-}$ | −71.46(11) |
| p$K$(−1tr/−2tr) | 5.20 | $[Cu_4H_{-13}L]^{10-}$ | −83.12(12) |
| p$K$(−2tr/−3tr) | 7.01 | p$K$(−4te/−5te) | 6.64 |
| p$K$(−3tr/−4tr) | 7.49 | p$K$(−5te/−6te) | 8.11 |
| p$K$(−4tr/−5tr) | 8.59 | p$K$(−6te/−7te) | 8.29 |
| p$K$(−5tr/−6tr) | 9.10 | p$K$(−7te/−8te) | 9.04 |
| p$K$(−6tr/−7tr) | 9.70 | p$K$(−8te/−9te) | 9.68 |
| p$K$(−7tr/−8tr) | 11.05 | p$K$(−9te/−10te) | 10.43 |
| p$K$(−8tr/−9tr) | 11.63 | p$K$(−10te/−11te) | 10.54 |
| | | p$K$(−11te/−12te) | 11.32 |
| | | p$K$(−12te/−13te) | 11.66 |

[a] p$K$(n/m) values reflect the p$K$ values of copper(II) complexes.

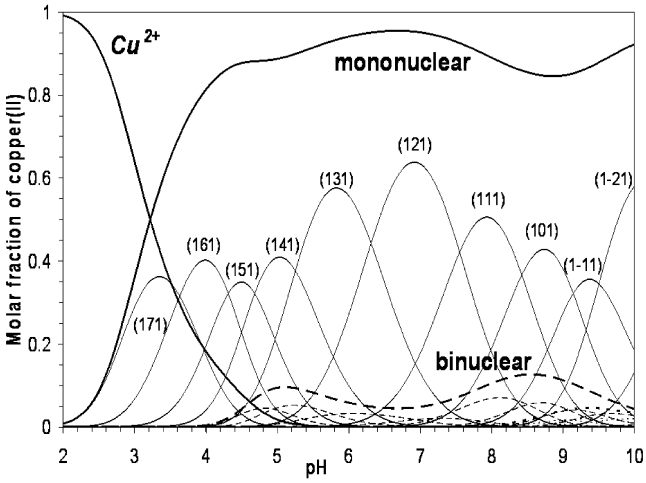


**Figure 5.** Species distribution of the complexes formed in the copper(II)−Aβ(1−16)PEG system ($c_{Cu(II)} = c_L = 2.0 \times 10^{-3}$ mol dm$^{-3}$).

have the highest p$K$ values, and their deprotonations take place in overlapping processes between pH 9 and 11. Protonation of the terminal amino groups takes place under slightly basic conditions (p$K$ = 7.69) and partially overlaps with the protonation processes of the three imidazole-N donor atoms. The average p$K$ value of these functions is 6.24, which is very close to the values reported for the small fragments in Table 1S. There are four carboxylate functions in the peptide, and their protonations significantly overlap, but γ-carboxylic groups of glutamic acid are generally less acidic than those of aspartic acid.

The pH-metric titration of the copper(II)−Aβ(1−16)PEG system revealed that the peptide is able to keep 4 equiv of copper(II) ions in solution even under strongly alkaline conditions. A computer evaluation of the data was performed with the consideration of mono- to tetranuclear complexes that confirmed this finding. The stability constants are listed in Table 2, and the speciation is shown in Figure 5.

These present results contradict previous potentiometric studies[52−54] concerning the copper(II)−Aβ(1−16) system where the metal complex formation processes have been described by the formation of mononuclear species. However, the low concentration of peptide used in the ESI-MS experiments allowed the present authors to show, in addition to the formation of mononuclear species, the existence of di-, tri-, and tetranuclear complexes (see Table 6S in the Supporting Information). Similarly, the ESI-MS study of copper(II)−Aβ(1−16)PEG also indicates a complex stoichiometry identical to that obtained by potentiometric titrations (data not shown).

The formation of oligonuclear complexes is, however, not surprising if one takes into account the complex formation processes of the short fragments Aβ(1−6) and Ac-Aβ(8−16)Y10A. It is clear from Tables 1S and 4S that both N- and C-terminal fragments are able to form dinuclear complexes, and it is also obvious that in the hexadecapeptide the metal binding sites of these fragments are well-separated, providing a good chance for the formation of even tetranuclear complexes. To reduce the number of possible metal binding sites, another derivative of the hexadecapeptide

**Table 3.** Protonation Constants (log $\beta_{pqr}$) and pK Values of the Aβ(1−16) and Aβ(1−16)Y10A Peptides ($T$ = 298 K, $I$ = 0.2 mol dm$^{-3}$ KCl)

| Species | log $\beta_{pqr}$ (L = Aβ(1−16)) | log $\beta_{pqr}$ (L = Aβ(1−16)Y10A) |
|---|---|---|
| $[HL]^{4-}$ | 10.46(1) | 10.31(1) |
| $[H_2L]^{3-}$ | 20.12(1) | 18.11(2) |
| $[H_3L]^{2-}$ | 27.88(1) | 25.13(2) |
| $[H_4L]^{-}$ | 34.86(1) | 31.60(3) |
| $[H_5L]$ | 41.27(1) | 37.57(3) |
| $[H_6L]^{+}$ | 47.24(1) | 42.26(4) |
| $[H_7L]^{2+}$ | 51.94(1) | 46.19(5) |
| $[H_8L]^{3+}$ | 55.93(2) | 49.67(5) |
| $[H_9L]^{4+}$ | 59.45(2) | 52.37(8) |
| $[H_{10}L]^{5+}$ | 62.25(3) | - |
| p$K$(Lys-$NH_2$/Tyr-OH) | 10.46 | 10.31 |
| p$K$(Tyr-OH/ Lys-$NH_2$) | 9.66 | - |
| p$K$(terminal-$NH_2$) | 7.76 | 7.80 |
| p$K$(imidazole of His6, His13 and His14) | 6.98 | 7.02 |
| | 6.41 | 6.47 |
| | 5.97 | 5.97 |
| p$K$(−COOH of Glu3 and Glu11) | 4.70 | 4.69 |
| | 3.99 | 3.93 |
| p$K$(−COOH of Asp1 and Asp7) | 3.52 | 3.48 |
| | 2.80 | 2.70 |

**Table 4.** Stability Constants (log $\beta_{pqr}$) of the Mononuclear Copper(II) Complexes with Aβ(1−16) and Aβ(1−16)Y10A peptides ($T$ = 298 K, $I$ = 0.2 mol dm$^{-3}$ KCl)[a]

| Species | log $\beta_{pqr}$ ($L$ = Aβ(1−16)) | log $\beta_{pqr}$ ($L$ = Aβ(1−16)Y10A) |
|---|---|---|
| $[CuH_7L]^{4+}$ | 54.67(4) | |
| $[CuH_6L]^{3+}$ | 51.01(2) | 44.79(7) |
| $[CuH_5L]^{2+}$ | 46.87(2) | 41.11(5) |
| $[CuH_4L]^{+}$ | 42.24(1) | 36.97(2) |
| $[CuH_3L]$ | 36.84(1) | 32.09(2) |
| $[CuH_2L]^{-}$ | 30.44(1) | 26.55(2) |
| $[CuHL]^{2-}$ | 22.78(1) | 19.84(3) |
| $[CuL]^{3-}$ | 14.43(1) | 12.07(4) |
| $[CuH_{-1}L]^{4-}$ | 5.42(1) | 3.42(4) |
| $[CuH_{-2}L]^{5-}$ | −4.38(1) | −5.88(4) |
| $[CuH_{-3}L]^{6-}$ | −14.88(2) | −16.55(5) |
| p$K$(7/6) | 3.66 | |
| p$K$(6/5) | 4.14 | 3.68 |
| p$K$(5/4) | 4.63 | 4.14 |
| p$K$(4/3) | 5.40 | 4.88 |
| p$K$(3/2) | 6.40 | 5.54 |
| p$K$(2/1) | 7.66 | 6.71 |
| p$K$(1/0) | 8.35 | 7.77 |
| p$K$(0/−1) | 9.01 | 8.65 |
| p$K$(−1/−2) | 9.80 | 9.30 |
| p$K$(−2/−3) | 10.50 | 10.67 |

[a] p$K$(n/m) values reflect the p$K$ values of copper(II) complexes.

Aβ(1−16) was synthesized in which Tyr10 is replaced by an Ala residue. Its complex formation processes were compared to those of the native tyrosine counterpart Aβ(1−16) (the p$K$ values of these ligands and the stability constants of their mononuclear copper(II) complexes are reported in Tables 3 and 4).

The different number of protonation sites and different charge of the same species make it difficult to compare the equilibrium data of Aβ(1−16) and Aβ(1−16)Y10A. However, the most protonated species $[CuH_7L]^{4+}$ was formed only with Aβ(1−16), supporting the hypothesis that phenolate is also protonated in the copper(II) species in the acidic pH range. This is a common feature of all tyrosyl-containing peptides but does not exclude the metal binding of phenolate in neutral or basic solutions. The formation of a Cu(II)−O-(phenolate) bond is, however, generally accompanied by the appearance of new charge transfer band in the 350−400 nm

range.[76] The existence of such a band either in the CD or UV−vis spectra was not observed at any pH value for any of the systems studied. The stringent similarity between CD spectra of the copper(II) complexes with the mutated A$\beta$(1−16)Y10A and the wild-type peptide fragment indicates that the phenolate of A$\beta$(1−16) is not a metal binding site in these complexes. Similar observations were reported for the $\varepsilon$-amino groups of lysyl residues, and their metal ion coordination was ruled out in the small peptide fragments of amyloid peptides and also for the copper(II) complexes of large prion fragments when high numbers of uncoordinated lysyl residues are present in the histidine-containing peptides.[68−70] As a consequence, the lysyl ammonium and tyrosyl phenolic groups can be considered as protonated side chains in any species existing below pH 8, and their deprotonation occurs only in parallel with the free ligand. Otherwise, the spectroscopic parameters of the various species formed in the copper(II)−A$\beta$(1−16) and A$\beta$(1−16)-Y10A systems are very similar to those of the copper(II)−A$\beta$-(1−16)PEG system; therefore, the binding modes will be discussed for the latter.

One of the most important findings from Figure 5 is linked to the existence of oligonuclear species at any metal ion-to-ligand ratio including equimolar solutions. Similar observations have already been reported for the copper(II) complexes of the 31-mer peptide fragments of prion protein Hu-PrP(84−114) containing three histidyl residues.[77] It was explained by the independent metal binding of each histidyl residue, when the statistical distribution of copper(II) among these functions resulted in the ratios 44.4%, 44.4%, and 11.1% for the mono-, di-, and trinuclear species, respectively.[77] In the case of amyloid peptides, there are four separated metal binding sites, and the statistical ratios of the various oligomers in equimolar samples are 42.2%, 42.2%, 14.1%, and 1.5% for the mono, di-, tri-, and tetranuclear complexes, respectively. The results obtained for the small fragments, however, revealed that the binding sites of A$\beta$(1−16)PEG are not equivalent. Supporting these results, the speciation curves shown in Figure 5 clearly indicate that the ratio of oligonuclear species is much less than the above-mentioned statistical values. This finding can also be explained taking into account that, (1) in the case of A$\beta$(1−16)PEG, there are three possible histidine binding sites, but their thermodynamic stabilities are lower than those of copper(II) species formed by the N-terminal amino group, and (2) the high number of coordinating side chains in the A$\beta$(1−16)PEG contributes to the enhanced stability of the mononuclear species formed with the N-terminal amino group in the form of macrochelates.

A model calculation was performed also for the copper-(II)−A$\beta$(1−6)−Ac-A$\beta$(8−16)Y10A mixed ligand system containing the same binding sites in separated molecules. In this case, the statistical distribution of the copper among the mono-, di-, tri-, and tetranuclear species was, however, weighted by the different affinities of A$\beta$(1−6) and Ac-A$\beta$(8−16)Y10A toward copper(II). This calculation uses also the stability constant values of the copper(II)−A$\beta$(1−6) and −Ac-A$\beta$(8−16)Y10A systems and therefore includes all possible coordination modes of the A$\beta$(1−16)PEG except distant macrochelation. The results of this calculation are shown in Figure 6 and reveal that the dinuclear complexes are present in comparable concentration in the measured systems (Figure 5) and in the statistically treated systems (Figure 6).

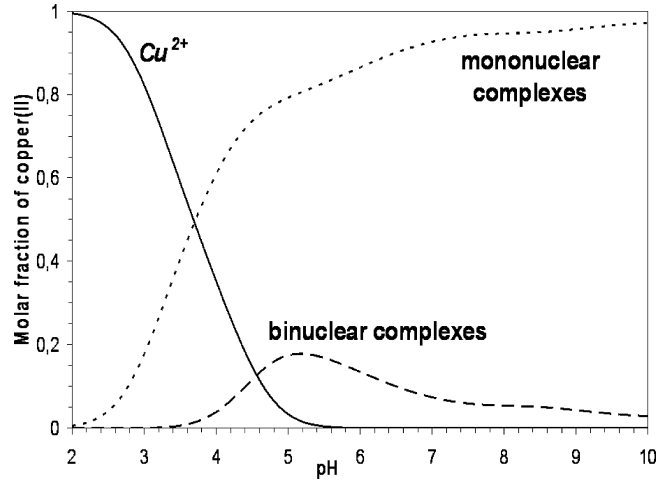


**Figure 6.** Species distribution of the complexes formed in the copper(II)−A$\beta$(1−6)−Ac-A$\beta$(8−16)Y10A system ($c_{Cu(II)} = c_L = 2.0 \times 10^{-3}$ mol dm$^{-3}$).

Both Figures 5 and 6 suggest that the mononuclear species predominate in the slightly acidic pH range when the formation of the six-membered ($NH_2$,$COO^-$) chelate from the Asp1 residue is the governing factor of complexation. CD spectral measurements unambiguously show that CD extrema cannot be observed below pH 6 (see Figure 9S in the Supporting Information), confirming that the N-terminal Asp residue is the primary metal binding site. A similar phenomenon was observed for the small fragments A$\beta$(1−4) and A$\beta$(1−6). Thus, the coordination modes of the protonated species containing two to seven protons ($[CuH_7L]^{4+}$ to $[CuH_2L]^-$) can be characterized by the ($NH_2$,$COO^-$) chelate supported by the macrochelation from the carboxylate and imidazole functions. The stability constants for the chelation at the N-terminus can be calculated taking into account the p$K$ values of the protonated residues. For this calculation, the coordination of aspartyl amino and carboxylate functions is assumed, while the lysyl, tyrosyl, and increasing number of histidyl residues are protonated. The values log $K$ = 7.77, 8.68, 9.82, and 10.24 were obtained for the species $[CuH_5L]^{2+}$, $[CuH_4L]^+$, $[CuH_3L]$, and $[CuH_2L]^-$, respectively. In the case of $[CuH_5L]^{2+}$, all of the above-mentioned donor functions are protonated, and the stability constants agree well with those of $\beta$-alanine or the small fragments of amyloid peptides. The deprotonation of histidyl side chains results in a significant increase of these equilibrium data supporting the macrochelation via these residues. Absorption maxima of the d−d band of equimolar samples in the pH range 4.5−7 (where the species $[CuH_5L]^{2+}$ to $[CuH_2L]^-$ predominate) progressively moved from 700

(76) Kiss, T.; Szücs, Z. J. *Chem. Soc. Dalton Trans.* **1986**, 2443–2447.
(77) Ösz, K.; Nagy, Z.; Pappalardo, G.; Di Natale, G.; Sanna, D.; Micera, G.; Rizzarelli, E.; Sóvágó, I. *Chem.−Eur. J.* **2007**, *13*, 7129–7143.

to 620 nm, in agreement with the suggested coordination mode.

Further increase of the pH, however, results in a significant blue shift of the absorption spectra and the appearance of CD extrema characteristic of peptide amide-bonded copper(II) complexes. It is also clear from the speciation curves that the involvement of amide binding is accompanied by the preferred formation of oligonuclear species. This can be easily understood if one takes into account that the coordination of a second metal ion at a histidyl and the neighboring amide sites breaks the macrochelate, and as a consequence, the metal binding affinity of the various locations will be more comparable. It is also important to note that there are several possibilities for the formation of coordination isomers, because the N-terminus and all three histidyl sites can be considered as potential binding sites. The UV−vis spectral parameters of coordination isomers are rather similar because at high pH all of them are 4N complexes in the form of ($NH_2$,$N^-$,$N^-$,$N^-$) or ($N_{im}$,$N^-$,$N^-$,$N^-$) coordination modes. As a consequence, the pH dependencies of the absorption spectra of the samples containing copper(II) and Aβ(1−16)PEG in different ratios are very similar to each other. The absorption maxima at high pH are always around 510−520 nm, while the molar absorptivities calculated for total copper(II) content are constant ($\varepsilon \sim 150\ M^{-1}\ cm^{-1}$), suggesting that all metal ions are in 4N-coordinated complexes.

Analysis of the CD spectra (see Figure 9S in the Supporting Information) provides more information about the existence of coordination isomers. The differences of CD spectra at 1:1 and 1:3 ligand-to-metal ratios are rather small, and even the pH dependence data support the existence of one major species in the whole pH range. This is, however, only a simplified interpretation (or misinterpretation) of the results, because the measured spectra are the superimposition of several parallel processes. The 1:1 spectra reveal that d−d transitions can be observed only above pH 7, while the Cu(II)−$N^-$(amide) charge transfer bands start to develop around pH 5.5−6. This strongly supports the idea that the amide coordination starts from the N-terminus, but the intensity of CD extrema is very small for the 2N and 3N complexes. It means that both ($NH_2$,$COO^-$) and ($NH_2$,$N^-$) coordination modes can exist below pH 7, and their stability is even enhanced by the formation of macrochelates, as discussed above. At the same time, the macrochelate suppresses the chance for the independent binding of side-chain imidazoles. As a consequence, the formation of 3N complexes is negligible because the pH range of their formation is around 6 for the small fragments. CD spectra of the ($N_{im}$,$N^-$,$N^-$)-coordinated 3N complexes exhibit a characteristic positive Cotton effect at 550 nm, which cannot be seen under any condition in the copper(II)−Aβ(1−16)PEG system. The increasing number of metal ions in the oligonuclear species also shifts the deprotonation of the amide functions to higher pH ranges, as can be seen from p*K* values reported in Table 2. This effect can be explained by the increasing negative charge of the various species at high pH.

As a consequence, the d−d bands of CD spectra demonstrate only the formation of 4N complexes, but it is also clear that they can be present in both possible coordination modes even in equimolar samples. The results for Aβ(1−4) revealed that the species with ($NH_2$,$N^-$,$N^-$,$N^-$) coordination are characterized by a simple negative Cotton effect at 515 nm. On the other hand, the ($N_{im}$,$N^-$,$N^-$,$N^-$) coordination modes at the histidyl sites exhibit both positive and negative Cotton effects at 650 and 505 nm, respectively. Taking into account the large overlap of the negative bands, it is impossible to calculate the exact distribution of these coordination modes to the overall spectra. However, the comparison of the spectra of Aβ(1−4) and Ac-Aβ(1−6) with those of Aβ(1−16)PEG helps to estimate these data. Namely, the ratios of the intensities of the negative (at 505 nm) and positive bands (at 650 nm) are 1.52 and infinity for the copper(II)−Ac-Aβ(1−6) and −Aβ(1−4) systems, respectively, while it is 2.6 for the copper(II)−Aβ(1−16)PEG system. These data unambiguously prove that both coordination modes exist in comparable concentrations in the latter system even in equimolar samples.

## Conclusions

The N-terminal region of Aβ has been shown to be flexible and accessible within amyloid fibrils.[78,79] Therefore, it constitutes an attractive therapeutic target, as illustrated by the ability of monoclonal antibodies directed toward this region to dissociate amyloid fibrils.[80,81] Indeed, only the antibodies raised against the N-terminal part of Aβ are able to reduce the plaque burden and restore cognitive deficits in the mouse model of AD.[82,83] It has also been shown that Aβ(1−16) zinc binding induces an agonist effect on the 4−10 epitope recognition by different monoclonal antibodies, suggesting a folding of the peptide that would render the epitope more accessible.[84] More recently, it has been reported that the dendrimeric Aβ(1−15) is an effective immunogen in wild-type and APP-tg mice.[85]

Because clinical testing for passive immunization has started, it is of major importance to characterize the structural changes of the N-terminal region of Aβ upon metal binding.

The combined application of both potentiometric and spectroscopic techniques was used to characterize the solution equilibria and binding modes of major species formed in the copper(II)−Aβ(1−16)PEG system. The interpretation of the data required also the synthesis and study of small peptide

(78) Petkova, A. T.; Ishii, Y.; Balbach, J. J.; Antzutkin, O. N.; Leapman, R. D.; Delaglio, F.; Tycko, R. *PNAS* **2002**, *99*, 16742–16747.
(79) Kheterpal, I.; Williams, A.; Murphy, C.; Bledsoe, B.; Wetzel, R. *Biochemistry* **2001**, *40*, 11757–11767.
(80) McLaurin, J.; Cecal, R.; Kierstead, M. E.; Tian, X.; Phinney, A. L.; Manea, M.; French, J. E.; Lambermon, M. H. L.; Darabie, A. A.; Brown, M. E.; Janus, C.; Chishti, M. A.; Horne, P.; Westaway, D.; Fraser, P. E.; Mount, H.T. J.; Przybylski, M.; St George-Hyslop, P. *Nat. Med.* **2002**, *8*, 1263–1269.
(81) Frenkel, D.; Balass, M.; Solomon, B. *J. Neuroimmunol.* **1998**, *88*, 85–90.
(82) Frenkel, D.; Dewachter, I.; Van Leuven, F.; Solomon, B. *Vaccine* **2003**, *21*, 1060–1065.
(83) Chauhan, N. B.; Siegel, G. J. *Neurosci. Lett.* **2005**, *375*, 143–147.
(84) Zirah, S.; Stefanescu, R.; Manea, M.; Tian, X.; Cecal, R.; Kozin, S. A.; Debey, P.; Rebuffat, S.; Przybylski, M. *Biochem. Biophys. Res. Commun.* **2004**, *321*, 324–328.
(85) Seabrook, T. J.; Thomas, K.; Jiang, L.; Bloom, J.; Spooner, E.; Maier, M.; Bitan, G.; Lemere, C. A. *Neurobiol. Aging* **2007**, *28*, 813–823.

**Scheme 3.** Schematic Representation of the Possible Binding Modes of the Major Complex Species Starting from the N-Terminus (a) Followed by the Formation of Macrochelates with the Histidines (b); Proposed Structure of $[Cu_2H_{-4}L]^{5-}$, when the Amino Terminus and His13 Are Independent Metal Binding Sites (c); and Proposed Structure of $[Cu_4H_{-11}L]^{8-}$, when the Amino Terminus and Three Histidyl Residues Are Independent Metal Binding Sites (d)

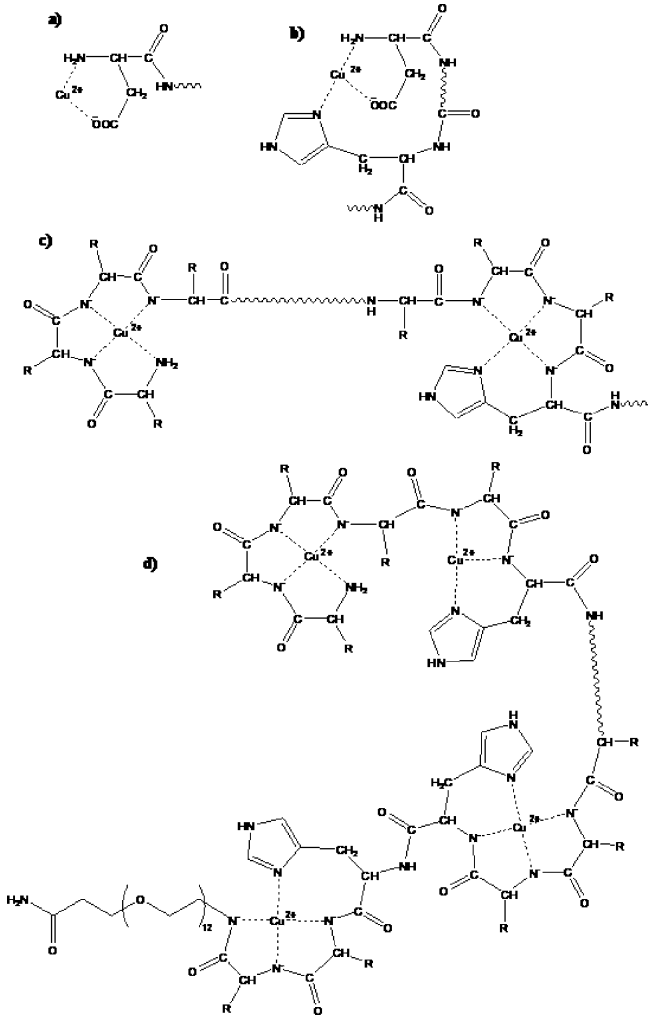

fragments representing the independent metal binding sites of the 16-mer peptide. The most important feature of the complex formation of the A$\beta$(1−16)PEG system comes from the formation of oligonuclear complexes indicating that the peptide has four independent metal binding sites. As a consequence, the ligand can keep as many as four equivalents of metal ions in solution even under strongly alkaline conditions. The high complexity of the speciation curves and the high number of different coordination isomers did not make it possible to structurally characterize all of the metal complexes, but the binding modes of the major species were elucidated, as shown by Scheme 3.

All data unambiguously prove that the N-terminus of the peptide is the major metal binding site, starting with the involvement of terminal amino and carboxylate functions of aspartyl residue in coordination (Scheme 3a). The identity of the oxygen donor atoms has been debated extensively, with proposals ranging from tyrosine at position 10[46,49,50] to one of several carboxylate side chains.[55,86,87] The copper(II) complexes with the mutated A$\beta$(1−16)Y10A show similar stability constant values as those of the analogues copper(II) complexes with the wild-type peptide (see Table 4). In addition, the same spectroscopic features (Figure 8S and 9S) have been found for the metal complexes both with A$\beta$(1−16)Y10A and with A$\beta$(1−16)PEG in the whole pH range investigated. Thus, we can conclude that the tyrosine residue is not involved in the copper(II) binding of the N-terminus fragment of the A$\beta$ peptide. The deprotonation of side-chain imidazole functions results in the formation of macrochelates of which several isomers exist, because one or more histidyl residues can occupy the remaining coordination sites (Scheme 3b). A further increase of pH results in the deprotonation and metal ion coordination of the amide functions subsequent to the amino group. The final species is a 4N complex with a ($NH_2$,$N^-$,$N^-$,$N^-$) coordination mode, which is a single species with the small tetrapeptide fragment A$\beta$(1−4), but it is formed in overlapping processes with the histidyl sites in the case of A$\beta$(1−16)PEG. Scheme 3c illustrates the binding modes of a dinuclear species when the amino terminus and His13 are the metal binding sites. However, it is important to emphasize that several coordination isomers of this dinuclear species can exist because any of the three histidyl residues can be the anchoring site. The exclusive binding of histidyl residues is also possible, although a preference for the coordination via the N-terminus is found. 2N and 3N coordinated complexes can also be detected, especially with the small peptide fragments. The high stabilities of the macrochelates of the hexadecapeptide (Scheme 3b), however, suppress the formation of these complexes, and they represent only minor species with A$\beta$(1−16)PEG.

To summarize, the results presented here clearly indicate that the N-terminus is the primary copper(II) binding site, especially in slightly acidic solution. The histidyl residues are in competition for copper(II) binding with the amino terminus upon increasing the pH, but the latter remains a possible binding site at any pH value. As a consequence, the coordination at the terminal amino group will be the governing process under physiological conditions, that is, around pH 7 and in the presence of ligand excess. In any case, it is important to emphasize the high affinity of the peptide for copper(II) binding in the form of mono- to tetranuclear complexes. Aggregation of the amyloid $\beta$ peptide causes deposits of insoluble A$\beta$ fibrils in the brain. However, recent results suggest that the soluble oligomeric species of $A\beta^{88-91}$ rather than the insoluble forms are the key toxic agents in AD. The soluble portion of A$\beta$ in the brain has

(86) Rickard, G. A.; Gomez-Balderas, R.; Brunelle, P.; Raffa, D. F.; Rauk, A. *J. Phys. Chem. A* **2005**, *109*, 8361–8370.
(87) Guilloreau, L.; Damian, L.; Coppel, Y.; Mazarguil, H.; Winterhalter, M.; Faller, P. *J. Biol. Inorg. Chem.* **2006**, *11*, 1024–1038.
(88) Klaim, W. L.; Krafft, G. A.; Finch, C. E. *Trends Neurosci.* **2001**, *24*, 219–224.
(89) Lashuel, H. A.; Hartley, D.; Petre, B. M.; Walz, T.; Lansbury, P. T., Jr. *Nature* **2002**, *418*, 291.
(90) Hoshi, M.; Sato, M.; Matsumoto, S.; Noguchi, A.; Yasutake, K.; Yoshida, N.; Sato, K. *Proc. Natl. Acad. Sci. U.S.A.* **2003**, *100*, 6370–6375.
(91) Cleary, J. P.; Walsh, D. M.; Hofmeister, J. J.; Shankar, G. M.; Kuskowski, M. A.; Selkoe, D. J.; Ashe, K. H. *Nat. Neurosci.* **2005**, *8*, 79–84.

been shown to be a better predictor of the severity of AD.[92] Cu(II) has been reported both to be a neuroprotectant[36,93] and to induce the formation of toxic A$\beta$ structures.[94] A$\beta$ neurotoxicity induced by Cu(II) has been suggested to result from changes in the coordination of the metal ion during A$\beta$ oligomerization or from different peptide/metal ratios;[95] however, these two possibilities are currently being debated.[96] On the other hand, EPR spectra collected by varying the A$\beta$ fibrilization time do not show any significant difference, indicating that the Cu(II) coordination environment does not depend on the A$\beta$ oligomeric state.[96] Moreover, Raman spectra of soluble complexes (Cu(II)/ligand = 4/1) collected at physiological pH and spectra of insoluble aggregates obtained in the pH range 5.8−6.6 have been reported to result from different coordination modes.[97] The solubility of the pegylated peptide allows for the distinction between the Cu(II) complex species forming at different pH values as well as for the determination of the binding affinity of the various metal complexes, which overcomes the uncertainties due to scarcely reliable speciations.

The present results may also help to explain the reasons for both the destabilization of large soluble aggregates and fibrilization resulting from different metal/ligand ratios or different pH values.

**Acknowledgment.** This work was supported by MiUR PRIN 2006-33492, 2005-035582, FIRB RBNE03PX83 and FIRB RBIN04L28Y (E.R.), the MTA(Hungary)-CNR(Italy) bilateral program and OTKA T048352 and D048488 (Hungary). The authors thank Mrs. Tiziana Campagna for technical assistance.

**Supporting Information Available:** Additional figures and tables. This material is available free of charge via the internet at http://pubs.acs.org.

IC8006052

(92) Lue, L. F.; Kuo, Y. M.; Roher, A. E.; Brachova, L.; Shen, Y.; Sue, L.; Beach, T.; Kurth, J. H.; Rydel, R. E.; Rogers, J. *Am. J. Pathol.* **1999**, *155*, 853–862.
(93) Yoshiike, Y.; Tanemura, K.; Murayama, O.; Akagi, T.; Murayama, M.; Sato, S.; Sun, X.; Tanaka, N.; Takashima, A. *J. Biol. Chem.* **2001**, *276*, 32293–32299.
(94) Kirkitadze, M. D.; Bitan, G.; Teplow, D. B. *J. Neurosci. Res.* **2002**, *69*, 567–577.
(95) Smith, D. P.; Cicciotosto, G. D.; Tew, D. J.; Fodero-Tavoletti, M. T.; Johanssen, T.; Masters, C. L.; Barnham, K. J.; Cappai, R. *Biochemistry* **2007**, *46*, 2881–2891.
(96) Karr, J. W.; Szalai, V. A. *Biochemistry* **2008**, *47*, 5006–5016.
(97) Hatcher, L. Q.; Hong, L.; Bush, W. D.; Carducci, T.; Simon, J. D. *J. Phys. Chem. B* **2008**, *112*, 8160–8164.